Stress-Induced Dynamic Regulation of Mitochondrial STAT3 and Its Association with Cyclophilin D Reduces Mitochondrial ROS Production

Jeremy A. Meier[9,10,#], Moonjung Hyun[10,#], Marc Cantwell[9,10], Ali Raza[8,10], Claudia Mertens[1], Vidisha Raje[10], Jennifer Sisler[10], Erin Tracy[2], Sylvia Torres-Odio[3], Suzana Gispert[3], Peter E. Shaw[4], Heinz Baumann[2], Dipankar Bandyopadhyay[7], Kazuaki Takabe[5,6,8,10], Andrew C. Larner[10,*]

[1]Laboratory of Molecular Cell Biology, The Rockefeller University, New York, NY 10065, [2]Department of Molecular and Cellular Biology, Roswell Park Cancer Institute, Buffalo, NY 14263, [3]Exp. Neurology, Goethe University Medical School, Frankfurt am Main, Germany, [4]School of Life Sciences, University of Nottingham, UK, [5]Division of Breast Surgery, Department of Surgical Oncology, Roswell Park Cancer Institute, Buffalo, NY 14263, [6]Department of Surgery, University at Buffalo Jacobs School of Medicine and Biomedical Sciences, the State University of New York, Buffalo, NY 14203, [7]Department of Biostatistics, [8]Division of Surgical Oncology, [9]Center for Clinical and Translational Research, [10]Department of Biochemistry and Molecular Biology and the Massey Cancer Center, Virginia Commonwealth University School of Medicine, Richmond, Virginia, 23298, USA
#These authors contributed equally to this work
*To whom correspondence should be addressed: andrew.larner@vcuhealth.org

ABSTRACT

Signal Transducer and Activator of Transcription 3 (STAT3) has been tied to various physiological and pathological functions, mainly as a transcription factor that translocates to the nucleus upon tyrosine phosphorylation induced by cytokine stimulation. In addition, a small pool of STAT3 resides in the mitochondria where it serves as a sensor for various metabolic stressors including reactive oxygen species (ROS). Mitochondrially-localized STAT3 largely exerts its effects through direct or indirect regulation of the activity of the electron transport chain (ETC). It has been assumed that STAT3 amounts in the mitochondria are static. We showed that various stimuli, including oxidative stress and cytokines, triggered a signaling cascade that resulted in a rapid loss of mitochondrially-localized STAT3. Recovery of the mitochondrial pool of STAT3 over time depended upon phosphorylation of Ser^{727} in

STAT3 and new protein synthesis. Under these conditions, mitochondrially-localized STAT3 also became competent to bind to cyclophilin D (CypD). Binding of STAT3 to CypD was mediated by the N-terminus of STAT3, which was also important for reducing mitochondrial ROS production after oxidative stress. These results outline a role for mitochondrially-localized STAT3 in sensing and responding to external stimuli.

INTRODUCTION

Signal Transducer and Activator of Transcription 3 (STAT3), a member of the STAT family of nuclear transcription factors, plays a key role in the regulation of a diverse set of physiological processes. Ideally situated as a molecular link between cellular inputs and nuclear gene regulation, STAT3 is aberrantly regulated under various pathological conditions including cancer, cardiovascular disease, and disorders in immune responses. The intricacies of this signaling network have been teased out to better appreciate the mechanisms behind STAT3's regulation of nuclear gene expression. The discovery of a distinct pool of STAT3 that resides in the mitochondria (1, 2) has added a new layer to the importance of STAT3 in controlling cellular homeostasis.

The functional importance of mitochondrial STAT3 (mitoSTAT3) has been extensively explored. MitoSTAT3 has been linked to control of the electron transport chain (ETC) and ATP production, mitochondrial encoded RNA regulation, modulation of reactive oxygen species generation, Ras transformation, cellular growth, and protection from ischemia-reperfusion injuries through regulation of the mitochondrial permeability transition pore (MPTP) (3). Most reports attribute phosphorylation of STAT3 at Ser^{727} as being key for its mitochondrial role with the MEK-ERK signaling axis potentially

being an important player (4, 5). However, the signaling pathways that control mitoSTAT3 largely still remain to be elucidated. Understanding of such a pathway is especially important considering that most studies looking to target STAT3 for therapeutic purposes have neglected its mitochondrial role, which could partly explain the absence of a clinically usable STAT3 inhibitor(6, 7). To more effectively study and target mitoSTAT3 we sought to examine its regulation at the signaling level.

We report that mitoSTAT3 was dynamically regulated by various cellular inputs, including oxidative stress and cytokines. Under these conditions mitoSTAT3 abundance initially decreased. This was followed by a re-equilibration of STAT3 into the mitochondria that depended upon Ser^{727} phosphorylation. During this recovery phase, mitoSTAT3 bound to cyclophilin D (CypD), which could play a role in stabilizing the mitoSTAT3 pool. The N-terminus of mitoSTAT3 appeared to be necessary for its association with CypD, thereby pointing to an additional site besides Ser^{727} in STAT3 that is important for its mitochondrial function. In this system the N-terminus of STAT3 also was important for regulating mitochondrial superoxide production following an oxidative insult, likely as a consequence of the CypD association. These results provide insight into a signaling pathway that controls the amount of mitoSTAT3, manipulation of which may provide new therapeutic modalities to treat diseases associated with dysfunctional actions of STAT3.

RESULTS

Rapid Loss of Mitochondrial STAT3 following an Oxidative Stress Insult

MitoSTAT3 limits mitochondrial and cellular ROS production(8-12). STAT3 is also post-translationally modified by oxidation that in turn regulates its function (13, 14) and ROS may be important for controlling mitoSTAT3 amounts (15). Therefore, we examined whether mitoSTAT3 was regulated following an oxidative insult. When wild-type MEFs or 4T1 breast cancer cells were treated with H_2O_2 we observed an initial loss of STAT3 from the mitochondria that recovered with time (**Figure 1A**). No changes were noted in STAT3 amounts in cytosolic fractions from H_2O_2 treated wild-type MEFs or 4T1 cells (**Figure 1B**), suggesting against nonspecific degradation of mitoSTAT3 as being responsible for the loss of the protein. H_2O_2 also induced phosphorylation of STAT3 at both Tyr^{705} and Ser^{727} (**Supplemental Figures 1A and B**), which was accompanied by an increase in the nuclear amounts of STAT3 (**Supplemental Figure 1C**). The loss of mitoSTAT3 upon treatment with H_2O_2 was concentration dependent and also coincided with activation of mitochondrial extracellular signal-regulated kinase 1 and 2 (ERK1/2) (**Figure 1C**). We noted potent Ser^{727} phosphorylation of mitoSTAT3 following H_2O_2 treatment (**Supplemental Figure 1D**), but mutation of either Ser^{727} or Tyr^{705} did not abolish the decrease in mitoSTAT3 amounts (**Supplemental Figure 1E**).

The kinetics of this pathway were extremely rapid because treatment with H_2O_2 for only 7.5 min. triggered a loss of mitoSTAT3, with recovery starting to occur by 30 min. (**Figure 1D**). The loss of mitoSTAT3 appeared to be specific as mitochondrial STAT1 (mitoSTAT1) amounts were unchanged following H_2O_2 treatment (**Figure 1D**). Probing mitochondrial extracts with a diverse set of STAT3 antibodies targeted to both the N- and C-terminus all showed the same loss of mitoSTAT3 upon H_2O_2 treatment making it unlikely that STAT3 was modified such that it is no longer immunoreactive

(**Supplemental Figure 1F**). Treatment of MDA-231 ($ER^-/PR^-/HER2^-$) or SK-BR3 ($ER^-/PR^-/HER2^+$) human breast cancer cell lines with H_2O_2 led to a similar loss of mitoSTAT3 (**Figure 1E**) indicating that this pathway is active in receptor negative and receptor positive cancer lines alike. Mitochondria isolated from WI-38 human lung fibroblasts that were immediately lysed after treatment with H_2O_2 also displayed a decrease in mitoSTAT3 (**Figure 1F**). This result suggested that it was unlikely that mitoSTAT3 was going into an insoluble fraction in the mitochondria and pointed to a true loss of the protein from this organelle. It appeared from these experiments and others (**Supplemental Figure 1G**) that the exact timing of the loss and recovery was cell dependent.

Loss and Recovery of MitoSTAT3 with Cytokine Administration

Because STAT3 is activated by IL-6 family cytokines, which bind to their respective receptor and transduce signals through gp130, we investigated whether typical STAT3 stimuli produce similar effects on mitoSTAT3. Treatment of MEFs with Oncostatin M (OSM) triggered a loss of mitoSTAT3 within minutes that again recovered with time (**Figure 2A**). Similar results were obtained when cells were treated with IL-6 with no apparent decrease in cytosolic STAT3 amounts (**Figure 2B**). We observed the loss and recovery of mitoSTAT3 with cytokine treatment in several mouse and human cell lines (**Figure 2C, Supplemental Figure 2A**). Longer-term treatment of cells with cytokines (16) or growth factors (5, 17, 18) drives an increase in mitochondrial STAT3 amounts. This effect was also re-capitulated in MEFs stimulated with OSM for 2H suggesting that acute and long-term exposure differentially regulated mitoSTAT3

(**Supplemental Figure 2B**). Likewise, extended treatment of cells with buthionine sulfoximine (BSO), an inhibitor of γ-glutamylcysteine synthetase that with time triggers oxidative stress, also led to an increase in mitoSTAT3 (**Supplemental Figure 2C**).

The above results implied that signals originating from the plasma membrane could be transduced to the mitochondria. To further explore this possibility we took advantage of cell lines containing chimeric receptors expressing the extracellular domain of granulocyte colony stimulating factor (GCSF) coupled intracellularly to gp130(19). Treatment with GCSF produced the same loss of mitoSTAT3 and subsequent recovery (**Figure 2D**). This mitochondrial signaling pathway was not exclusively driven by gp130 coupled stimuli because interferon β (IFNβ), a type I interferon that activates STAT3, also caused a loss of mitoSTAT3 (**Supplemental Figure 2D**). Not all stimuli activate this cascade because interferon γ (IFNγ) (**Supplemental Figure 2E**) and epidermal growth factor (EGF) (**Supplemental Figure 2F**) failed to substantially decrease mitoSTAT3. To minimize contamination from the cytosol and other organelles crude mitochondria used in these studies were always trypsinized to remove external proteins. We further purified mitochondria over a percoll gradient (20) to separate the mitochondria from the tightly linked mitochondrial associated membranes (MAM). Under these conditions, mitoSTAT3 still decreased with OSM treatment (**Figure 2E,** P-mito) confirming a loss of STAT3 selectively from the mitochondrial fraction. This pathway could also be functionally relevant *in vivo,* but may be difficult to fully explore because mice injected with saline alone display a robust decrease in mitoSTAT3 amounts, likely due to stress pathways induced by injecting the animal (**Supplemental**

Figure 2G). Together these results show that mitoSTAT3 is dynamically regulated by various stressors.

JAK Inhibition and mitoSTAT3 Loss Following Cytokine Treatment

Since the JAK receptor associated tyrosine kinases drive downstream signaling from the IL-6 family cytokines and interferons, we tested whether inhibition of JAK kinase activity prevented the loss of mitoSTAT3. Pre-treatment of MEFs with the pan-JAK inhibitor Ruxolitinib potently suppressed the loss of mitoSTAT3 induced with either OSM (**Figure 3A**) or IL-6 (**Supplemental Figure 3A**). Ruxolitinib did not inhibit H_2O_2-induced loss of mitoSTAT3 (**Figure 3B**), which can likely bypass receptor mediated activation and act on other downstream signaling cascades. These results were mirrored in MDA-231 cells pre-incubated with Ruxolitinib and then subjected to either OSM or H_2O_2 treatment (**Figure 3C**). Inhibition of STAT3 directly through its SH2 domain with the small molecule cryptotanshinone also did not substantially suppress OSM induced mitoSTAT3 loss (**Supplemental Figure 3B**). This finding is consistent with prior reports that demonstrate that the SH2 domain is dispensable for mitoSTAT3's actions (1, 2, 11). Cryptotanshinone also blocks Tyr^{705} phosphorylation of STAT3 and consistent with our results using Y705F STAT3 mutants (**Supplemental Figure 1E**) it would appear that Tyr^{705} is not involved in the mitochondrial localization of STAT3 after stimulation.

We explored possible downstream mediators that transduce the signal(s) to the mitochondria from OSM and H_2O_2. Notably, H_2O_2 produced a robust increase in mitochondrial ROS production that was not seen with OSM (**Figure 3D**). Considering

that STAT3 can be regulated by oxidative modifications (21) and various signaling pathways can be activated independently of upstream events in the presence of ROS (22), we tested whether antioxidants could block the loss of mitoSTAT3 with H_2O_2 treatment. The mitochondrial targeted antioxidant mitoTEMPO (23) did not suppress the H_2O_2 induced decrease in mitoSTAT3 (**Figure 3E**) likely ruling out an oxidative driven program.

Further evaluation of the signaling pathway driving mitoSTAT3 loss revealed that Ruxolitinib inhibited ERK activation induced by OSM, but not by H_2O_2. STAT3, and in particular mitoSTAT3, has been linked to regulation by the MEK-ERK pathway (4), and mitoSTAT3 amounts may be controlled by this cascade (5). The MEK inhibitor PD0325901 completely blocked H_2O_2 mediated activation of ERK, but did not prevent mitoSTAT3 loss (10 min. H_2O_2 treatment) or its initial recovery (30 min. H_2O_2 treatment) (**Figure 3F**). This result suggested that the MEK-ERK pathway was dispensable for these actions on mitoSTAT3, or alternatively, that there was compensation from another signaling cascade. Treatment with the broad-spectrum kinase inhibitor staurosporine or the protein kinase inhibitor H7 dihydrochloride also did not block mitoSTAT3 loss (**Supplemental Figure 3C**). H7 inhibits kinase A (PKA) and protein kinase C (PKC), both of which have been implicated in mitoSTAT3 biology (17, 24). Other signaling cascades converge on STAT3 including p38, PI3K/Akt, JNK, and mTOR (25). Targeting each of these pathways individually did not prevent mitoSTAT3 loss (**Supplemental Figures 3D-G**). These results imply that multiple signaling events, which likely complement each other, may affect mitoSTAT3 making identification of the downstream regulation of this pathway challenging. Though the pharmacological inhibitors used in

these studies have other cellular effects, the lack of a response in terms of blockade of the mitoSTAT3 loss lends greater support to the complexity of this signaling cascade.

Although we observe H_2O_2 and cytokine induced loss of mitoSTAT3 in most cell lines, those with low basal amounts of mitoSTAT3, as in the case of the human breast cancer cell line MCF-7, often failed to show any further reduction in mitochondrial levels of STAT3 (**Supplemental Figure 3H**). This is consistent with tight regulation of mitoSTAT3 levels and cell line and context dependent stimulation of the pathway.

Role of Ser^{727} Phosphorylation and New Protein Synthesis on mitoSTAT3 Recovery

Because we could not definitively link a kinase pathway with the decreases in mitoSTAT3 following a stimulus, we investigated the potential contribution of signaling driven proteolysis as a mechanism behind mitoSTAT3 regulation. Consistent with this idea, *$STAT3^{-/-}$* MEFs expressing a mitochondrially targeted STAT3 and treated with H_2O_2 showed the same loss of STAT3 in whole cell extract samples as from mitochondrial fractions (**Figure 4A**). Though not statistically significant, the trend suggested that the mitoSTAT3 loss could be due to protein degradation rather than export of STAT3 from the mitochondria and trafficking to another compartment, but we cannot exclude this latter possibility. STAT3 is cleaved by proteases such as caspases (26) and calpains (27), the latter of which is active in the mitochondria (28). However, treatment with the calpain inhibitor MDL-28170 did not block H_2O_2 induced mitoSTAT3 loss (**Supplemental Figure 4A**).

Within the mitochondria, protein degradation is driven by two key serine proteases, Lon protease and ClpP Protease, which are essential for mitochondrial protein

quality control (29). We utilized the synthetic triterpenoid CDDO-Me to target Lon protease, which inhibits its proteolytic activity in cells (30, 31). Pre-treatment with CDDO-Me also did not block the loss of mitoSTAT3 following an oxidative stress insult (**Supplemental Figure 4B**). The general proteasome inhibitor MG132, which also inhibits Lon protease and attenuates proteasome-mediated outer mitochondrial membrane degradation (32), failed to block the decrease in mitoSTAT3 seen with either OSM or H_2O_2 (**Figure 4B**). Similarly, primary *ClpP*$^{-/-}$ MEFs treated with OSM and H_2O_2 still demonstrated loss of mitoSTAT3 (**Supplemental Figure 4C**).

Because degradation may play a role in mitoSTAT3 regulation, we tested whether or not protein synthesis was needed to drive full recovery of mitoSTAT3 amounts. Inhibition of protein synthesis with cycloheximide reduced the return of mitoSTAT3 following either OSM or H_2O_2 treatment in MDA-231 cells (**Figures 4C and D**). Similar results were obtained from H_2O_2 treated wild-type MEFs incubated with cycloheximide (**Supplemental Figure 4D**). However, cycloheximide pre-treatment had little effect on the cytoplasmic pool of STAT3 (**Supplemental Figure 4E**) making it more likely that cycloheximide may be affecting the chaperone protein that targets STAT3 to the mitochondria. We also cannot exclude the possibility that there is a specific mitochondrial pool of STAT3 that is selectively affected by cycloheximide under these conditions, or alternatively, that cycloheximide affects some component of the signaling pathway through an off-target effect. Ser^{727} phosphorylation of STAT3 is important for STAT3's trafficking to the mitochondria and may at least partially regulate its import (33). As such, we speculated that mutation of Ser^{727} to alanine (S727A) would also negatively affect the re-equilibration of mitoSTAT3 following its loss from the

mitochondria. *STAT3*$^{-/-}$ MEFs expressing S727A STAT3 did not recover to the same extent as *STAT3*$^{-/-}$ MEFs expressing STAT3α after 30' OSM treatment and amounts of mitoSTAT3 only starting to normalize after 1H of treatment in S727A mutant-expressing *STAT3*$^{-/-}$ MEFs (**Figures 4E and F**). These results provide insight into the regulation of mitoSTAT3 and provide a system through which the signaling pathways controlling STAT3 and its mitochondrial localization can be more effectively explored.

Interaction of mitoSTAT3 with Cyclophilin D

mitoSTAT3 has been previously linked to regulation of the mitochondrial permeability transition pore, potentially through an interaction with Cyclophilin D (CypD) (34). Like other members of the cyclophilin family, CypD is a peptidyl-prolyl isomerase that triggers the opening of the permeability transition pore(35). It is also an important therapeutic target for ischemia-reperfusion injuries. Prolyl isomerase proteins mediate proper folding of target proteins, thus affecting protein stability, localization, and activity (36). Inhibition of CypD with Cyclosporine A (CsA) drives an unfolded protein response pointing to a crucial role of CypD as a chaperone protein (37). Likewise, deletion of CypD impairs the function of several mitochondrial proteins (38, 39).

We noted that STAT3 became competent to bind to CypD after 15' to 30' of H_2O_2 treatment (**Figure 5A**), which corresponds with re-recruitment of STAT3 to the mitochondria following mitoSTAT3 loss (**Figure 1D**). This result was confirmed in purified mitochondrial extracts incubated with recombinant GST-CypD from H_2O_2-treated wild-type MEFs (**Figure 5B**) and 4T1 cells (**Figure 5C**). In wild-type MEFs, mitoSTAT3 associated with CypD after 30' of H_2O_2 treatment, which was maintained

until 2-4H after stimulation when mitoSTAT3 amounts had returned to baseline (**Figure 5B,** Input bottom panel). Notably, binding of mitoSTAT3 to GST-CypD was maintained out to 4H in 4T1 mitochondrial lysates, likely reflecting the longer time it takes for mitoSTAT3 to re-equilibrate following its loss after H_2O_2 treatment (**Figure 1A**). Incubation of cells with the CypD inhibitor CsA blocked the association of mitoSTAT3 with CypD making a non-specific interaction between these proteins less likely (**Figures 5B and C**). Similar results were seen in mitochondria from *STAT3*$^{+/+}$ or *STAT3*$^{-/-}$ MEFs treated with H_2O_2 (**Supplemental Figure 5A**). Incubation with GST alone did not pull down any detectable mitoSTAT3, further supporting a specific interaction (**Figure 5D**). Immunoprecipitation of STAT3 from mitochondrial lysates from wild-type MEFs, 4T1 cells, or MDA231 breast cancer cells treated for 30' with H_2O_2 also showed an increased association between mitoSTAT3 and CypD compared to untreated controls (**Figure 5E** and **Supplemental Figures 5B and C**). Binding of mitoSTAT3 to CypD in IL-6-treated MDA-231 cells and various OSM-treated cell lines coincided with the recovery phase of mitoSTAT3 following stimulation (**Figure 5F** and **Supplemental Figures 5D-F**). These results suggest that upon STAT3's re-entry to the mitochondria it binds to CypD, potentially as part of its import and proper folding mechanism.

The N-terminus of STAT3 as key for CypD Binding

Aside from being critical for the actions of mitoSTAT3, Ser^{727} in STAT3 may also be necessary to facilitate binding to CypD (34). We evaluated whether mutation of Ser^{727} affected STAT3's interaction with CypD. GST-CypD pulldown of either 293T cells or *STAT3*$^{-/-}$ MEFs extracts expressing STAT3 S727A or 4T1 cells expressing

STAT3 Y705F/S727A or Y705F/S727D variants revealed that Ser^{727} did not affect STAT3-CypD binding (**Supplemental Figures 6A -C**). Mutation of $Ser^{727}$to the phospho-mimetic aspartic acid (S727D) seemed to increase basal association of STAT3 with CypD, potentially reflecting that increased Ser^{727} phosphorylation of STAT3 may promote this protein-protein interaction. However, STAT3β, a natural occurring splice variant that lacks the Ser^{727} site, bound to CypD following H_2O_2 treatment (**Supplemental Figure 6D**) suggesting that Ser^{727} was dispensable for the binding of STAT3 to CypD.

To further evaluate how STAT3 interacts with CypD we used mitoSTAT1, which did not bind to CypD (**Supplemental Figure 6E**). Using chimeric STAT3:STAT1 proteins (13, 40) expressed in 293T cells we mapped the region of STAT3 that was necessary for the H_2O_2 induced STAT3-CypD interaction to the N-terminus of STAT3 (amino acids 1-330 of STAT3) (**Figures 6A and B**). This result was validated with constructs that contain the N-terminus of STAT3 (STAT3/1S) and those with the N-terminus of STAT1 and the remaining STAT3 C-terminal portion (STAT1/3S) (**Figure 6C**). To further examine the mechanism behind this association, we developed a cell free system that used solubilized cell extracts warmed to 30^{o}C. STAT3 bound to CypD in extracts from both 293T cells over-expressing STAT3 and from purified mitochondria from MDA-231 cells with endogenous STAT3 (**Figures 6D and E**). In both cases, binding of STAT3 to CypD was inhibited in the presence of CsA, and STAT3 was not detectable in lysates incubated with GST alone (**Figures 6D and E**). This cell free system provides a useful tool to interrogate the regulation of the interaction of mitoSTAT3 and CypD in future studies.

Role of a Tyrosine Phosphatase in mitoSTAT3-CypD Interactions

Utilizing the cell free system for studying the binding of mitoSTAT3 to CypD we sought to further explore the mechanism driving this protein-protein interaction. Because warming of the extracts was sufficient to drive the association of these two proteins, we hypothesized that some enzymatic activity was required. Incubation of extracts with the tyrosine phosphatase inhibitor vanadate (Na_3VO_4) prevented the inducible binding of STAT3 to CypD to the same extent as a pan-phosphatase inhibitor (PhosSTOP) (**Figure 6F**), which also contains serine/threonine phosphatase inhibitors. A role for a tyrosine phosphatase in this pathway seemed likely because the serine/threonine phosphatase inhibitor calycunin A did not affect this interaction (**Figure 6F**). These results were confirmed in cells pre-treated with vanadate, which blocked the H_2O_2 induced binding of STAT3 to CypD (**Figure 7A**). In cell extracts subjected to λ phosphatase treatment (**Figure 7A**), STAT3 bound to CypD to a greater extent, further supporting a role for dephosphorylation. Dialysis of cell extracts to remove small molecules, like ATP, did not affect mitoSTAT3's interaction with CypD pointing to an ATP-independent mechanism for this interaction (**Figure 7B**). Similarly, incubation of the kinase inhibitor Staurosporine in extracts did not prevent the association of mitoSTAT3 with CypD (**Figures 7A and B**). Together, these results point to a role of a tyrosine phosphatase in mediating mitoSTAT3 binding to CypD.

We examined if STAT3 was the target of the tyrosine phosphatase and needed to be modified to interact with CypD. STAT3 added to whole cell extract *STAT3*$^{-/-}$ MEFs that were then incubated at 30^{o}C bound to CypD (**Figure 7C**). However, STAT3 added

after extracts were warmed and then placed on ice did not bind to CypD (**Figure 7C**). This result suggested that STAT3 needs to be present during the stimulation and that STAT3 itself is likely modified to interact with CypD.

Importance of the STAT3-CypD Association

The absence of either STAT3 or CypD compromises mitochondrial metabolism and overall mitochondrial health (41-43). Because STAT3 associates with CypD upon its return to the mitochondria, we hypothesized that the chaperone function of CypD might be important for the stability of mitoSTAT3. MitoSTAT3 amounts were similar in $CypD^{+/+}$ and $CypD^{-/-}$ MEFs following cytokine treatment (**Supplemental Figure 6F**) with the latter at times showing a slight delay in full restoration of mitoSTAT3. Pre-treatment with CsA did not affect mitoSTAT3's signaling regulation, suggesting that CypD is not involved in the loss or initial recovery of mitoSTAT3 after H_2O_2 or cytokine treatment (**Figure 7D and Supplemental Figure 6G**). As CsA also prevents permeability transition, opening of the mitochondrial permeability transition pore (MPTP) and its sequelae is unlikely to be an important driving force in the observed loss of mitoSTAT3 with external stimuli.. However, these results do not completely address whether or not CypD is ultimately required for the stability of mitoSTAT3 as changes in the acute setting may only reflect whether or not STAT3 is appropriately targeted and imported into the mitochondria. In some instances, there appeared to be decreased basal amounts of mitoSTAT3 in the absence of CypD or after CsA treatment (**Figure 7D and Supplemental Figures 6F-G).** Based on the sensitivity of the full recovery of mitoSTAT3 to cycloheximide (**Figure 4C**) we examined whether cells lacking CypD

relied more heavily on protein synthesis to maintain mitoSTAT3 amounts. MitoSTAT3 amounts decreased in *CypD*$^{-/-}$ MEFs treated with cycloheximide more readily than *CypD*$^{+/+}$ MEFs (**Figure 7E**). These results suggest that CypD may be an important binding partner and regulator of mitoSTAT3 stability, most likely through facilitating STAT3's proper folding once it reaches the mitochondria.

To examine the functional role of the STAT3-CypD association we took advantage of the link between mitoSTAT3 and reactive oxygen species production. MitoSTAT3 limits mitochondrial and cellular ROS generation (8-12). We speculated that the N-terminus of STAT3 would be essential for contributing to this protective effect due to its association with CypD. *STAT3*$^{-/-}$ MEFs generated more mitochondrial superoxide production than their wild-type counterparts after an oxidative stress (**Figure 7F)**. Reconstitution of *STAT3*$^{-/-}$ MEFs with either wild-type STAT3 or the chimeric STAT3/1S construct that contains the N-terminus of STAT3 restored superoxide amounts to wild-type amounts (**Figure 7F)**. These results implicate the N-terminus of STAT3, which mediates STAT3's binding to CypD, as being important in limiting stress induced mitochondrial ROS generation. As we have not evaluated the role of wild-type STAT1 in this system, we can't definitely exclude the possibility that the C-terminus of STAT1 is not contributing at least in part to the ROS mitigating effect observed with the STAT3/1S construct. However, considering the well-established function of STAT3 in mitochondrial ROS regulation (8-12), we anticipate that the majority of the observed decrease in superoxide production with re-expression of full-length STAT3 is driven by its N-terminus based on the comparable results seen with the 3/1S chimera.

DISCUSSION

mitoSTAT3 affects the ETC, ATP production, mitochondrial ROS generation, mtDNA regulation, mitochondrial Ca^{2+} content, and MPTP susceptibility. Together this regulation drives both normal biological processes and pathological states. We now add to and extend those findings by describing a signaling pathway that acutely regulates mitoSTAT3 and drives its association with CypD (**Figure 8**).

MitoSTAT3 is implicated in both cardioprotection in ischemia-reperfusion injuries (9, 34, 44-46) and transformation and growth of cancer cells (2, 11, 47-49). Understanding how mitoSTAT3 is regulated will be a valuable tool to more effectively target the full STAT3 program driving these pathological states. This is especially important because the majority of STAT3 inhibitors designed to date target STAT3's SH2 domain, which likely would not affect mitoSTAT3's activity as the SH2 domain is dispensable for its mitochondrial function (1, 2). Certain pharmacological treatments affect mitoSTAT3 abundance, though their widespread use in manipulating the mitochondrial STAT3 pathway remains to be determined(49, 50). For instance, phospho-valproic acid limits the translocation of mitoSTAT3 in a pancreatic cancer cell model, which leads to increased cancer cell death (49), pointing to the value in targeting mitoSTAT3.

STAT3's mitochondrial localization can be altered during cell differentiation (15, 16), with ROS being one mechanism to decrease mitoSTAT3 (15). Increased mitoSTAT3 amounts drive T-cell activation and axonal growth in cells under chronic stimulation with cytokines(16) and growth factors (5, 18). Together with the results presented here, these reports would suggest that mitoSTAT3 is differentially regulated in

the acute compared to chronic setting. MitoSTAT3 is important in the proliferation of embryonic stem cells, where it supports oxidative phosphorylation to couple STAT3's transcriptional effects with maintaining pluripotency (51). Fine-tuning mitoSTAT3 amounts then is likely important in controlling mitochondrial adaptation to the real-time cellular demands, suggesting that this pathway is a crucial regulatory step in normal biological processes as well.

Currently, the fate of mitoSTAT3 following stimulation is unknown. Proteolysis of mitoSTAT3 is consistent with the kinetics of its loss from the mitochondria. We detected proteolytic fragments of STAT3 in the mitochondria but not in cytoplasmic extracts suggesting, but not proving, the observed loss of mitoSTAT3 was due to proteolysis. Various inhibitors of mitochondrial proteases did not prevent the loss of mitoSTAT3. It is possible that these inhibitors do not enter the mitochondria efficiently, or the protease that cleaves mitoSTAT3 is insensitive to the inhibitors used. Intriguingly, both p50 and IκBα is lost from the mitochondria following stimulation with TNFα, with IκBα likely being degraded following phosphorylation in part by a calpain-dependent mechanism (52). STAT3's degradation may be linked with its phosphorylation status (53) and calpains target and cleave STAT3(27). However, calpain inhibition did not affect on treatment-induced mitoSTAT3 loss. Pharmacological blockade of Lon and deletion of ClpP proteases, which are serine proteases in the mitochondria, did not attenuate mitoSTAT3's loss. Other mitochondrial proteases, including inner membrane associated mitochondrial AAA proteases, which are emerging as important targets in mitochondrial protein quality control and dynamics (29) may be the primary driver of mitoSTAT3 loss. Simultaneous blockade of multiple protease pathways may be necessary to prevent

STAT3 cleavage as inhibition of a single cascade may lead to altered enzymatic activity and compensation by another protein. Consistent with this possibility, inhibition of only Lon protease in HeLa cells does not grossly change mitochondrial function or protein content due to increased activity from another ATP dependent protease (54). Another explanation for the loss of mitoSTAT3 is that it is removed from mitochondria following stimulation through the PINK1-Parkin dependent mitochondrial derived vesicle (MDV) pathway (55, 56). These vesicles remove damaged mitochondrial cargo for transport to the lysosome, and are critical to mitochondrial quality control (57). The mitochondrial protein Tom20 is trafficked through these MDVs, and STAT3 is reported to interact with Tom20 (34).

Our results demonstrate that aside from H_2O_2, which has broad effects on intracellular signaling cascades, cytokines also affected mitoSTAT3 suggesting that signals emanating from the plasma membrane were rapidly transduced to the mitochondria. We do not know what signaling cascade is responsible for H_2O_2- and cytokine-induced loss of STAT3 from the mitochondria. Although various kinases, including Akt, ERK, and JNK, have been reported to reside in the mitochondria where they regulate mitochondrial dynamics through phosphorylation events (58-60)(61), inhibition of these mitochondrial-localized signaling proteins in isolation did not affect stimulus dependent decreases in mitoSTAT3.

The dependence of the recovery of mitoSTAT3 after stimulation on Ser^{727} phosphorylation agrees with a prior report that demonstrated the Ser^{727} site is important for its mitochondrial import (33). The absence of an effect on basal mitoSTAT3 amounts when Ser^{727} is mutated to an alanine (S727A) suggests though, that there are likely other

means of bypassing this import requirement that are compromised under stress conditions. Like other proteins that are imported into mitochondria, the mitochondrial import of STAT3 requires an intact mitochondrial membrane potential (62). STAT3 is ultimately being targeted to the inner mitochondrial membrane or matrix (33, 34). Under stress conditions, a reduction in mitochondrial membrane potential disables the mitochondrial import machinery, which affects the import efficiency and mitochondrial abundance of various proteins (63, 64). However, continuous import of STAT3 to maintain its mitochondrial abundance is unlikely because mitoSTAT3 was remarkably stable in wild-type cells hours after cycloheximide treatment (**Figure 7E**). Although the MEK-ERK pathway phosphorylates STAT3 at Ser^{727} and has been linked to regulating mitoSTAT3(4, 5), MEK and ERK inhibition did not affect mitoSTAT3 abundance. This is not surprising because various other kinases can phosphorylate STAT3 at this residue, and there is likely a large degree of crosstalk between multiple signaling pathways. The full recovery of mitoSTAT3 was blunted when protein synthesis was inhibited, despite the large cytoplasmic pool of STAT3 that was still present under these conditions. These results suggest that either the chaperone protein that is responsible for the translocation of STAT3 to mitochondria has a short half-life or there is a limited fraction of STAT3 that can go to the mitochondria. The latter idea is interesting and could be analogous to p53, of which there is a distinct mitochondrial isoform (65). Other isoforms of STAT3 have been reported but to date there is no information on whether or not they, or others, are mitochondrially localized (66).

Based on the above results (**Figure 4**) we anticipate that mitoSTAT3's loss is likely due to proteolysis. However, a fraction of mitoSTAT3 could traffic to another

cellular compartment. Signaling to the nucleus would be an attractive target, considering STAT3's role as a nuclear transcription factor. Under the conditions which induced loss of mitoSTAT3, STAT3 was potently recruited to the nucleus making it at least plausible that the mitochondrial pool of STAT3 might contribute to the nuclear actions of STAT3. However, this possibility is difficult to assess because of high cytosolic abundance of STAT3. Other mitochondrial proteins, including the pyruvate dehydrogenase complex and SSBP1, can translocate from the mitochondria to the nucleus to regulate transcription under stress conditions (67, 68). This mitochondrial retrograde signaling event occurs in *Caenorhabditis elegans*, where the protein ATFS-1 links coordinate mitochondrial and nuclear programs (63, 69, 70). Intriguingly, ATFS-1 is also proteolyzed in the mitochondria and accumulates in the nucleus under stress conditions. A similar pathway has not been detected in mammalian cells, but it is thought that signaling molecules such as ROS or Ca^{2+} released from mitochondria might activate pathways (such as JNK) to drive mito-nuclear crosstalk (71). STAT3 not only modulates mitochondrial ROS production (9, 11, 12, 15, 45), but it also directly regulates mitochondrial calcium content(16). It is tempting to speculate that mitoSTAT3, as well as other transcription factors that localize to the mitochondria such as NFκB, might be part of this communication network, especially when one considers the dynamic regulation we have observed in mitoSTAT3. Whether this is through direct trafficking to the nucleus, or indirectly through regulation of intracellular ROS and Ca^{2+} content remains to be determined.

CypD plays a role in retrograde signaling through its effects on STAT3 activation (72). It is interesting then that mitoSTAT3 binds to CypD in an inducible manner. The

interaction of STAT3 and CypD coincides with mitoSTAT3's return to the mitochondria. Re-entry of proteins into the mitochondria requires their proper folding after mitochondrial import, and the chaperone function of CypD may play a critical role in this process. Indeed, the decreased mitoSTAT3 amounts in cells lacking CypD following cycloheximide treatment suggest that the stability of the mitoSTAT3 pool at least partly depends on CypD. mitoSTAT3 that is serine phosphorylated associates with CypD in cardiomyocyte mitochondria, where it plays a role in regulation of MPTP sensitivity (34). Surprisingly, we observed that Ser^{727} in STAT3, which has been implicated in its mitochondrial action, was not required for the binding of mitoSTAT3 to CypD. Rather, the N-terminus of STAT3 mediates the association suggesting that other domains in mitoSTAT3 are relevant for its non-canonical mitochondrial role. Interestingly, selective targeting of the N-terminus of STAT3 with peptide-based inhibitors affects mitochondrial membrane potential and lead to cancer cell death(73).

The action of a tyrosine phosphatase on STAT3 was necessary for its interaction with CypD. This is interesting as binding of STAT3 to CypD can be potently induced with H_2O_2, a stimulus that normally inhibits tyrosine phosphatases through oxidation of key cysteines in their catalytic pocket (74). A major regulator of STAT3 signaling is the Src homology-2 domain containing protein tyrosine phosphatase-2 (SHP2) (75). Coincidentally, SHP2 is also paradoxically activated by oxidative stress (76), and it can localize to the mitochondria where it regulates mitoSTAT3 (77). Future work will clarify the identity and role of this phosphatase in this signaling cascade.

Consistent with prior reports (8-12), we have demonstrated a role for STAT3 in the modulation of cellular ROS. We extend that work by demonstrating that the N-

terminus of STAT3 may be key for limiting mitochondrial ROS production after stress insult. Because the N-terminus of STAT3 was also the critical region for binding to CypD, we anticipate that the STAT3-CypD association is important for regulating ROS generation at the mitochondrial level. This could be through stabilization of the mitoSTAT3 pool allowing STAT3 to more effectively alter ETC activity under stress conditions as previously proposed (45). Increased amounts of mitoSTAT3 could also serve as a greater redox reserve effectively scavenging mitochondrial reactive oxygen species as they are generated (14). It is also conceivable that the association of mitoSTAT3 with CypD directly controls the opening of the mitochondrial permeability transition pore (34) that is closely linked to cellular redox status. Work is ongoing to better understand how this protein-protein interaction affects this functional endpoint. Tight regulation of cellular redox state is paramount during cellular transformation and progression of cancer. Interestingly, CypD is necessary for Ras transformation and tumorigenesis(78). Because mitoSTAT3 is necessary for Ras transformation (2) it is tempting to speculate that CypD's requirement in this process is through its binding and stabilization of the mitoSTAT3 pool. Further characterization of this cascade and how mitoSTAT3 is controlled is necessary to provide insight into how to effectively target the mitochondrial pool of STAT3 for the purposes of promoting health and combating disease.

MATERIALS AND METHODS

Cell Culture

The following cell lines were used in this study: Wild-type Mouse Embryonic Fibroblasts (MEFs), *STAT3*$^{-/-}$ MEFs, *CypD*$^{-/-}$ MEFs, *ClpP*$^{+/+}$ MEFs, *ClpP*$^{-/-}$ MEFs, 4T1 murine breast

adenocarcinoma cells, MDA-MB-231 triple negative human breast cancer cells, WI-38 human lung fibroblasts, SKBR3 $HER2^+$ human breast cancer cells, BT474 $HER2^+$ human breast cancer cells, MDA-MB-453 $HER2^+$ human breast cancer cells, 293T human embryonic kidney cells, HeLa human cervical cancer cells, and rat hepatoma cell lines expressing the GCSF-gp130 chimeric receptor. The human breast cancer cell lines were kindly provided by Drs. Gordon Ginder, Charles Clevenger, and Frank Fang, Virginia Commonwealth University. WI-38 human lung fibroblasts were provided by Dr. Swati Deb, Virginia Commonwealth University. HeLa cells were provided by Dr. Thurl Harris, University of Virginia. *CypD*$^{-/-}$ MEFs were kindly provided by Dr. Ute Moll, Stony Brook University. *ClpP*$^{+/+}$ and *ClpP*$^{-/-}$ MEFs were kindly provided by Dr. Georg Auburger, Goethe - Universität. Rat hepatoma cell lines were provided by Dr. Heinz Baumann, Roswell Park Cancer Institute. Cells were routinely grown in appropriate growth culture (DMEM, DMEM F-12, or RPMI) media supplemented with 10% heat inactivated Fetal Bovine Serum (Serum Source International, Charlotte, NC) and 50U/mL Penicillin and 50ug/mL Streptomycin (Life Technologies). Prior to experimental use cell lines were determined to be free of mycoplasma contamination.

Reagents

The following chemicals and inhibitors were used: Ruxolitinib (JAK inhibitor, 5μM, Selleck Chemicals), PD0325901 (MEK inhibitor, 10μM, Selleck Chemicals), LY294002 (PI3K inhibitor, 25μM, Cell Signaling), SB203580 (p38 MAPK inhibitor, 10μM, Calbiochem), SP600125 (JNK inhibitor, 50μM, Cell Signaling), Torin 1(mTOR inhibitor, 10μM, Tocris Biosciences), Cyclosporine A (Cyclophilin D inhibitor, 5μM or 10μg/mL, Sigma), Cycloheximide (Protein synthesis inhibitor, 50μg/mL, MP Biomedicals),

Staurosporine (Tyrosine Kinase inhibitor, 100nM, Sigma), H7 Dihydrochloride (Protein Kinase A/C/G inhibitor, 20μM, Sigma), Cryptotanshinone (STAT3 inhibitor, 10μM, Selleck Chemicals), mito-TEMPO (mitochondrial anti-oxidant, 100μM, Sigma), MG132 (Proteasome Inhibitor, 25μM, Tocris Biosciences), MDL-28170 (Calpain Inhibitor, 10μM, kind gift from Dr. Ed Lesnefsky, Virginia Commonwealth University, Richmond, VA) CDDO-Me (Lon Protease Inhibitor, 50μM, Sigma), recombinant murine IL-6 (50ng/mL, Peprotech), recombinant human IL-6 (50ng/mL, Peprotech), soluble human IL-6Rα (50ng/mL, Peprotech), human OSM with carrier (12.5ng/mL, Cell Signaling), mouse OSM with carrier (12.5ng/mL, Cell Signaling), Hydrogen Peroxide 30% Solution (1mM unless otherwise indicated, Sigma), cOmplete protease inhibitor cocktail (per manufacturer's instructions, Roche), phosSTOP phosphatase inhibitor cocktail (per manufacturer's instructions, Roche). All other chemicals used for buffer formulations were purchased from Sigma-Aldrich or Fisher Scientific unless otherwise indicated.

Treatments

All stimulations were carried out in cells cultured in full serum media (10%) so as to avoid any effect of serum starvation on mitoSTAT3 amounts. Aside from protease inhibitor studies (4H pre-treatment), all other inhibitors were pre-incubated on cells for no more than 1H prior to H_2O_2 or cytokine treatment. Vehicle or DMSO treatments were used when appropriate as controls.

Plasmids

pGEX-CypD was a kind gift from Dr. Ute Moll, Stony Brook University(79). pRC-CMV STAT3, pRC-CMV STAT1, pRC-CMV STAT3/1H, pRC-CMV STAT3/1S, pRC-CMV STAT1/3H, and pRC-CMV STAT1/3S have been described previously (13). MSCV-

IRES-GFP expression vectors containing STAT3α, STAT3β, STAT3 Y705F, STAT3 S727A, STAT3 S727D, MLS-STAT3 and the Phoenix helper construct have been previously described (1)

Transfections

Transfections were carried out with the use of FuGENE (Promega). Briefly, plasmid DNA (1-3μg) was combined with FuGENE reagent at a 1:3 ratio (μg:mL) and incubated in OPTI-MEM media for 5 minutes prior to adding to cells. For shRNA viral transductions, 293T cells were transfected via FuGENE with the indicated shRNA vector (1.5μg), pCMV-VSV-G envelope protein vector (1μg), and pCMV-dR8.2 dvpr packaging plasmid vector (1.5μg). Viral supernatants were collected after 48H, spun down, and filtered through a 0.45μm filter prior to adding to cells in the presence of 10μg/mL Polybrene (Millipore). MSCV retroviruses were similarly packaged in 293T cells following transfection with the appropriate MSCV viral vector (4μg) and the phoenix helper construct (1μg). Cell transductions were carried out for 24H in the presence of virus and after 48H puromycin selection (2μg/mL, shRNA experiments) or GFP FACS sorting was performed to generate a pure, stable pool of cells expressing the indicated viral vector.

Recombinant Proteins

pGEX-CypD and pGEX vectors were transformed into BL-21(DE3) competent bacteria. Bacterial clones containing the plasmid of interest were grown up overnight in 25mL of LB media and the following morning was diluted 1:15 into a 500mL culture. Bacteria were grown up until OD_{600} reached 0.6 at which point protein expression was induced with 1mM IPTG for 6H. The bacteria were pelleted and lysed in bacterial lysis buffer

followed by sonication. The bacterial cell extract was then incubated with glutathione sepharose 4B beads (GE Healthcare, #17-0756-01) for 1H at 4^{o}C. Bead bound GST proteins were pelleted and washed 3X in bacterial lysis buffer prior to storage at -80^{o}C. A portion of the purified proteins were resolved by SDS-PAGE and gels were fixed and Coomassie stained for quantification of GST recombinant proteins as compared to a BSA standard curve. Recombinant Flag-STAT3 protein was a kind gift from Claudia Mertens, Rockefeller University, Darnell Lab(80).

SDS-PAGE and Immunoblotting

Cell samples were lysed in 20mM HEPES, pH 7.4, 300mM NaCl, 10mM KCl, 1mM $MgCl_2$, 20% glycerol, and 1% Triton X-100. Equal protein was loaded on Tris-glycine gels and subjected to SDS-PAGE electrophoresis. Gels were transferred to PVDF membranes (Millipore, IPVH00010) using a semi-dry transfer apparatus. The following antibodies were used overnight at 4^{o}C with shaking following blocking for 1H in 5% milk or 5% BSA in 1X TBS + 0.1% Tween-20: STAT3 (Cell Signaling #9139, mouse monoclonal, clone 124H6), STAT3 (N-terminal, BD Biosciences, mouse monoclonal), STAT3 (Cell Signaling, rabbit polyclonal), pTyr^{705} STAT3 (Cell Signaling , mouse monoclonal), pSer^{727} STAT3 (Cell Signaling, rabbit polyclonal), Complex V Subunit I (Abcam, mouse monoclonal), STAT1 (BD Biosciences, mouse monoclonal), pTyr^{701} STAT1 (Cell Signaling, rabbit polyclonal), CypD (PPIF, Abcam, mouse monoclonal), Calreticulin (Cell Signaling, rabbit monoclonal), Histone H3 (Cell Signaling, mouse monoclonal), Lamin A/C (Cell Signaling, mouse monoclonal) ATP5O (Abcam, mouse monoclonal), GRIM19 (Abcam, mouse monoclonal), pAkt (Cell Signaling, rabbit polyclonal), pc-Jun (Cell Signaling, rabbit polyclonal), NDUFA9 (Abcam #ab14713,

mouse monoclonal), pERK1/2 (Cell Signaling #9101, rabbit polyclonal), Tubulin (Sigma #T8203, mouse monoclonal, α-Tubulin), Actin (Cell Signaling, mouse monoclonal) Secondary antibodies were used at a concentration of 1:5000 for 1H at room temperature in 5% milk in 1X TBS + 0.1% Tween-20.

After washing, blots were incubated with Amersham ECL (GE Healthcare, RPN2106) or ECL2 Western Blotting (Thermo-Scientific, 80196) chemiluminescent detection reagents and developed. Where indicated densitometry quantification was performed using ImageJ Software (Rasband, W.S., ImageJ, U. S. National Institutes of Health, Bethesda, Maryland, USA, http://imagej.nih.gov/ij/, 1997-2015).

Mitochondria Isolation

Pure mitochondria and mitochondria-associated membrane (MAM) fractions were isolated as previously described(81). For crude mitochondria adherent cells were treated and then washed with ice cold 1X PBS, trypsinized, and collected with ice cold full serum media. Cells were spun down for 5min. at 1000RPM and the pellets were washed 1x with 3mL's of ice cold 1X PBS. Cells were spun down again for 5min. at 1000RPM and the supernatant was aspirated. The cell pellets were resuspended in an appropriate volume (1-2mL's) of sucrose buffer (10mM HEPES, pH 7.4, 250mM sucrose, 1mM EDTA, protease and phosphatase inhibitors) and incubated on ice for 10min. Cells were then added to a douncer (all steps on ice) and cells were homogenized with manual strokes until roughly 90% of the cells were broken (verified with Trypan blue during douncing). Cells were collected and spun down for 5min. at 800g at 4^{o}C to pellet unbroken cells and nuclei. The supernatant was collected and spun down for 10min. at 8800g at 4^{o}C to pellet crude mitochondria. The supernatant was again collected and

transferred to a new tube labeled cytosolic fraction, which was spun down for 10min. at 10000g at 4°C to remove any contaminants from the cytosolic sample. After this spin the cytosolic supernatant (700µL) was transferred to a new tube and frozen at -80°C until further analysis. The crude mitochondrial pellet from above was resuspended in 490µL sucrose buffer and 10µL of a 5mg/mL stock solution of trypsin was added to each tube (for a final concentration of 100µg/mL). Samples were then rotated for 10min. at 4°C after which 500µL of a 5% BSA solution was added to each tube to inactivate the trypsin. Samples were again rotated for 1min. at 4°C and then spun down at 10000g for 10min. at 4°C. The supernatant was aspirated off (including the trypsin digested material surrounding the mitochondrial pellet) and the mitochondrial pellets were washed in 500µL of sucrose buffer 2X (spins done at 10000g for 10min. at 4°C). After the final wash the mitochondrial pellets were resuspended in an appropriate volume of sucrose buffer and stored at -80°C until further analysis. For protein analysis mitochondrial supernatants were lysed in an equal volume of sucrose buffer plus 1XPBS with 2% Triton X-100 plus protease and phosphatase inhibitors.

Pulldown Assays

Pulldown assays were performed as previously described(79). Briefly, recombinant bead-bound GST-CypD or GST alone was blocked in H-buffer (20mM HEPES pH 7.7, 1mg/mL BSA, 75mM KCl, 0.1mM EDTA, 2.5mM $MgCl_2$, 0.05% NP-40, 1mM DTT). 250µg of mitochondrial or whole cell extracts (lysed as described above) were incubated with 20µg of bead bound GST-CypD or GST alone and incubated overnight at 4°C. Beads were pelleted and washed in H-buffer and bound proteins were analyzed by immunoblotting.

Immunoprecipitation

Immunoprecipitation was carried out as previously described (82). Mitochondrial or whole cell extracts were incubated overnight at 4°C with an antibody against STAT3 (SantaCruz, sc-482, C-20, 1:100 dilution) plus agarose beads (Protein G Sepharose Fast Flow, GE Healthcare, 17-0618-01) or control IgG plus agarose beads in IP buffer (pH 7.4, 150 mM NaCl, 50mM Tris-HCl, 1% Triton, 1 mM EDTA with protease and phosphatase inhibitor cocktails (Roche, Indianapolis, IN). Immunoprecipitates were washed three times with wash buffer (150 mM NaCl, 50mM Tris-HCl, 1% Triton, protease and phosphatase inhibitor cocktails), and separated by SDS-PAGE with blotting against the indicated antibodies.

Cell Free System for studying mitoSTAT3-CypD Interactions

Mitochondria or whole cell extracts were prepared as described, but importantly in the absence of protease or phosphatase inhibitors. Lysates were incubated on ice or at 30^{o}C for 30 minutes in 1X NEBuffer for Protein Metallophosphatases (50mM HEPES, 10mM NaCl, 1mM $MnCl_2$, 2mM DTT, 0.01% Brij 35, pH 7.5). Following incubation, extracts (100μg) were subjected to GST-CypD pulldown as described. When applicable cell lysates were dialyzed for 3H using a 10,000MWCO dialyzer cassette according to the manufacturer's protocol (Slide-A-Lyzer, Thermo Fisher Scientific).

Animals

Animals were treated in compliance with the Guide for the Care and Use of Laboratory Animals under the protocols approved by Virginia Commonwealth University Institutional Animal Care and Use Committee.

Liver Mitochondrial Assays

8-12 week old male CD-1 mice (Charles River Laboratories) were tail vein injected with 500μg/kg recombinant murine IL-6 (Peprotech) and sacrificed at the indicated times. Livers were harvested from mice and washed with ice cold PBS. The livers were minced and homogenized in 10mL MSM (220mM Mannitol, 70mM Sucrose, 5mM MOPS) on ice. A homogenate fraction was collected for each sample and solubilized as described abover. Homogenized tissues were then centrifuged at 500xg for 10 minutes at 4°C to remove cell debris. The supernatants were centrifuged at 3700xg for 10 minutes at 4°C to pellet mitochondria. Mitochondria were re-suspended in 5mL of ice cold MSM-EDTA (MSM Buffer plus 2mM EDTA) and spun at 3700xg for 10 minutes at 4°C. Supernatants were discarded and the mitochondria were re-suspended in 2.5mL of MSM-EDTA buffer and spun down at 3700xg for 10 minutes at 4°C (83). Mitochondria in MSM-EDTA buffer were lysed via the addition of an equal volume of 2% Triton X-100 in 1X PBS with protease and phosphatase inhibitor cocktails and analyzed via immunoblotting.

Statistical Analysis

Results are presented as the mean ± SEM. The statistical analysis was carried out as follows. For Figures 1A and Supplementary Figure 1D, differences between the Control and the groups under comparison were assessed using a two-sided 2-sample t-test at 5% level of significance. For Figure 1D, differences between mitoSTAT3 and mitoSTAT1 at various times of H_2O_2 treatment were assessed using two-sided 2-sample t-test at 5% level of significance. For all others, the differences between groups were initially assessed using a one-way ANOVA, followed by false discovery rate (FDR) (84) adjusted multiple (pairwise) comparisons at a 5% threshold. If P values were < 0.05, we considered the group difference to be significant. N values are indicated in the figure

legends for each panel and always represent independent experiments. Representative blots are shown.

Supplementary Materials

Fig. S1: Ser^{727} and Tyr^{705} of STAT3 are Not Required for H_2O_2 Induced mitoSTAT3 Loss.

Fig. S2: Selectivity of the mitoSTAT3 Signaling Pathway and Relevance In Vivo

Fig. S3: Inhibition of Relevant Kinase Pathways does not Affect Stimulation Induced Decreases in mitoSTAT3.

Fig. S4: Inhibition of mitoProteases Does Not Affect Proteolysis of mitoSTAT3.

Fig. S5: mitoSTAT3 Inducibly Binds to CypD Following H_2O_2 or Cytokine Stimulation.

Fig. S6: Ser^{727} is Dispensable for the mitoSTAT3-CypD Interaction.

REFERENCES AND NOTES

1. J. Wegrzyn, R. Potla, Y. J. Chwae, N. B. Sepuri, Q. Zhang, T. Koeck, M. Derecka, K. Szczepanek, M. Szelag, A. Gornicka, A. Moh, S. Moghaddas, Q. Chen, S. Bobbili, J. Cichy, J. Dulak, D. P. Baker, A. Wolfman, D. Stuehr, M. O. Hassan, X. Y. Fu, N. Avadhani, J. I. Drake, P. Fawcett, E. J. Lesnefsky, A. C. Larner, Function of mitochondrial Stat3 in cellular respiration. *Science.* **323**, 793-797 (2009).

2. D. J. Gough, A. Corlett, K. Schlessinger, J. Wegrzyn, A. C. Larner, D. E. Levy, Mitochondrial STAT3 supports Ras-dependent oncogenic transformation. *Science.* **324**, 1713-1716 (2009).

3. J. A. Meier, A. C. Larner, Toward a new STATe: the role of STATs in mitochondrial function. *Semin. Immunol.* **26**, 20-28 (2014).

4. D. J. Gough, L. Koetz, D. E. Levy, The MEK-ERK Pathway Is Necessary for Serine Phosphorylation of Mitochondrial STAT3 and Ras-Mediated Transformation. *PLoS One.* **8**, e83395 (2013).

5. X. Luo, M. Ribeiro, E. R. Bray, D. H. Lee, B. J. Yungher, S. T. Mehta, K. A. Thakor, F. Diaz, J. K. Lee, C. T. Moraes, J. L. Bixby, V. P. Lemmon, K. K. Park, Enhanced Transcriptional Activity and Mitochondrial Localization of STAT3 Co-induce Axon Regrowth in the Adult Central Nervous System. *Cell. Rep.* (2016).

6. M. S. Wake, C. J. Watson, STAT3 the oncogene - still eluding therapy? *FEBS J.* **282**, 2600-2611 (2015).

7. R. Yang, M. Rincon, Mitochondrial Stat3, the Need for Design Thinking. *Int. J. Biol. Sci.* **12**, 532-544 (2016).

8. K. Szczepanek, Q. Chen, M. Derecka, F. N. Salloum, Q. Zhang, M. Szelag, J. Cichy, R. C. Kukreja, J. Dulak, E. J. Lesnefsky, A. C. Larner, Mitochondrial-targeted Signal transducer and activator of transcription 3 (STAT3) protects against ischemia-induced changes in the electron transport chain and the generation of reactive oxygen species. *J. Biol. Chem.* **286**, 29610-29620 (2011).

9. K. Boengler, E. Ungefug, G. Heusch, R. Schulz, The STAT3 Inhibitor Stattic Impairs Cardiomyocyte Mitochondrial Function Through Increased Reactive Oxygen Species Formation. *Curr. Pharm. Des.* (2013).

10. C. Lachance, S. Goupil, P. Leclerc, Stattic V, a STAT3 inhibitor, affects human spermatozoa through regulation of mitochondrial activity. *J. Cell. Physiol.* **228**, 704-713 (2013).

11. Q. Zhang, V. Raje, V. A. Yakovlev, A. Yacoub, K. Szczepanek, J. Meier, M. Derecka, Q. Chen, Y. Hu, J. Sisler, H. Hamed, E. J. Lesnefsky Jr, K. Valerie, P. Dent, A. C. Larner, Mitochondrial-Localized Stat3 Promotes Breast Cancer Growth via Phosphorylation of Serine 727. *J. Biol. Chem.* (2013).

12. D. J. Garama, T. J. Harris, C. L. White, F. J. Rossello, M. Abdul-Hay, D. J. Gough, D. E. Levy, A Synthetic Lethal Interaction between Glutathione Synthesis and Mitochondrial Reactive Oxygen Species Provides a Tumor-Specific Vulnerability Dependent on STAT3. *Mol. Cell. Biol.* **35**, 3646-3656 (2015).

13. L. Li, S. H. Cheung, E. L. Evans, P. E. Shaw, Modulation of gene expression and tumor cell growth by redox modification of STAT3. *Cancer Res.* **70**, 8222-8232 (2010).

14. M. C. Sobotta, W. Liou, S. Stocker, D. Talwar, M. Oehler, T. Ruppert, A. N. Scharf, T. P. Dick, Peroxiredoxin-2 and STAT3 form a redox relay for H2O2 signaling. *Nat. Chem. Biol.* **11**, 64-70 (2015).

15. A. H. Kramer, A. L. Edkins, H. C. Hoppe, E. Prinsloo, Dynamic Mitochondrial Localisation of STAT3 in the Cellular Adipogenesis Model 3T3-L1. *J. Cell. Biochem.* **116**, 1232-1240 (2015).

16. R. Yang, D. Lirussi, T. M. Thornton, D. M. Jelley-Gibbs, S. A. Diehl, L. K. Case, M. Madesh, D. J. Taatjes, C. Teuscher, L. Haynes, M. Rincon, Mitochondrial Ca(2)(+) and membrane potential, an alternative pathway for Interleukin 6 to regulate CD4 cell effector function. *Elife.* **4**, 10.7554/eLife.06376 (2015).

17. E. Macias, D. Rao, S. Carbajal, K. Kiguchi, J. DiGiovanni, Stat3 binds to mtDNA and regulates mitochondrial gene expression in keratinocytes. *J. Invest. Dermatol.* **134**, 1971-1980 (2014).

18. L. Zhou, H. P. Too, Mitochondrial localized STAT3 is involved in NGF induced neurite outgrowth. *PLoS One.* **6**, e21680 (2011).

19. H. Kim, T. S. Hawley, R. G. Hawley, H. Baumann, Protein tyrosine phosphatase 2 (SHP-2) moderates signaling by gp130 but is not required for the induction of acute-phase plasma protein genes in hepatic cells. *Mol. Cell. Biol.* **18**, 1525-1533 (1998).

20. M. R. Wieckowski, C. Giorgi, M. Lebiedzinska, J. Duszynski, P. Pinton, Isolation of mitochondria-associated membranes and mitochondria from animal tissues and cells. *Nat. Protoc.* **4**, 1582-1590 (2009).

21. P. E. Shaw, Could STAT3 provide a link between respiration and cell cycle progression? *Cell. Cycle.* **9**, 4294-4296 (2010).

22. M. Schieber, N. S. Chandel, ROS function in redox signaling and oxidative stress. *Curr. Biol.* **24**, R453-62 (2014).

23. A. E. Dikalova, A. T. Bikineyeva, K. Budzyn, R. R. Nazarewicz, L. McCann, W. Lewis, D. G. Harrison, S. I. Dikalov, Therapeutic targeting of mitochondrial superoxide in hypertension. *Circ. Res.* **107**, 106-116 (2010).

24. M. Dorsch, F. Behmenburg, M. Raible, D. Blase, H. Grievink, M. W. Hollmann, A. Heinen, R. Huhn, Morphine-Induced Preconditioning: Involvement of Protein Kinase A and Mitochondrial Permeability Transition Pore. *PLoS One.* **11**, e0151025 (2016).

25. J. S. Rawlings, K. M. Rosler, D. A. Harrison, The JAK/STAT signaling pathway. *J. Cell. Sci.* **117**, 1281-1283 (2004).

26. J. W. Darnowski, F. A. Goulette, Y. J. Guan, D. Chatterjee, Z. F. Yang, L. P. Cousens, Y. E. Chin, Stat3 cleavage by caspases: impact on full-length Stat3 expression, fragment formation, and transcriptional activity. *J. Biol. Chem.* **281**, 17707-17717 (2006).

27. A. Oda, H. Wakao, H. Fujita, Calpain is a signal transducer and activator of transcription (STAT) 3 and STAT5 protease. *Blood.* **99**, 1850-1852 (2002).

28. J. Thompson, Y. Hu, E. J. Lesnefsky, Q. Chen, Activation of mitochondrial calpain and increased cardiac injury: beyond AIF release. *Am. J. Physiol. Heart Circ. Physiol.* **310**, H376-84 (2016).

29. P. M. Quiros, T. Langer, C. Lopez-Otin, New roles for mitochondrial proteases in health, ageing and disease. *Nat. Rev. Mol. Cell Biol.* **16**, 345-359 (2015).

30. L. Gibellini, M. Pinti, R. Bartolomeo, S. De Biasi, A. Cormio, C. Musicco, G. Carnevale, S. Pecorini, M. Nasi, A. De Pol, A. Cossarizza, Inhibition of Lon protease by triterpenoids alters mitochondria and is associated to cell death in human cancer cells. *Oncotarget.* **6**, 25466-25483 (2015).

31. S. H. Bernstein, S. Venkatesh, M. Li, J. Lee, B. Lu, S. P. Hilchey, K. M. Morse, H. M. Metcalfe, J. Skalska, M. Andreeff, P. S. Brookes, C. K. Suzuki, The mitochondrial ATP-dependent Lon protease: a novel target in lymphoma death mediated by the synthetic triterpenoid CDDO and its derivatives. *Blood.* **119**, 3321-3329 (2012).

32. P. Bragoszewski, A. Gornicka, M. E. Sztolsztener, A. Chacinska, The ubiquitin-proteasome system regulates mitochondrial intermembrane space proteins. *Mol. Cell. Biol.* **33**, 2136-2148 (2013).

33. P. Tammineni, C. Anugula, F. Mohammed, M. Anjaneyulu, A. C. Larner, N. B. Sepuri, The import of the transcription factor STAT3 into mitochondria depends on GRIM-19, a component of the electron transport chain. *J. Biol. Chem.* **288**, 4723-4732 (2013).

34. K. Boengler, D. Hilfiker-Kleiner, G. Heusch, R. Schulz, Inhibition of permeability transition pore opening by mitochondrial STAT3 and its role in myocardial ischemia/reperfusion. *Basic Res. Cardiol.* **105**, 771-785 (2010).

35. J. W. Elrod, J. D. Molkentin, Physiologic functions of cyclophilin D and the mitochondrial permeability transition pore. *Circ. J.* **77**, 1111-1122 (2013).

36. K. P. Lu, X. Z. Zhou, The prolyl isomerase PIN1: a pivotal new twist in phosphorylation signalling and disease. *Nat. Rev. Mol. Cell Biol.* **8**, 904-916 (2007).

37. M. Hibino, K. Sugiura, Y. Muro, Y. Shimoyama, Y. Tomita, Cyclosporin A induces the unfolded protein response in keratinocytes. *Arch. Dermatol. Res.* **303**, 481-489 (2011).

38. T. T. Nguyen, R. Wong, S. Menazza, J. Sun, Y. Chen, G. Wang, M. Gucek, C. Steenbergen, M. N. Sack, E. Murphy, Cyclophilin D modulates mitochondrial acetylome. *Circ. Res.* **113**, 1308-1319 (2013).

39. S. Menazza, R. Wong, T. Nguyen, G. Wang, M. Gucek, E. Murphy, CypD(-/-) hearts have altered levels of proteins involved in Krebs cycle, branch chain amino acid degradation and pyruvate metabolism. *J. Mol. Cell. Cardiol.* **56**, 81-90 (2013).

40. L. Li, P. E. Shaw, A STAT3 dimer formed by inter-chain disulphide bridging during oxidative stress. *Biochem. Biophys. Res. Commun.* **322**, 1005-1011 (2004).

41. R. S. Carreira, Y. Lee, M. Ghochani, A. B. Gustafsson, R. A. Gottlieb, Cyclophilin D is required for mitochondrial removal by autophagy in cardiac cells. *Autophagy.* **6**, 462-472 (2010).

42. M. Tavecchio, S. Lisanti, M. J. Bennett, L. R. Languino, D. C. Altieri, Deletion of Cyclophilin D Impairs beta-Oxidation and Promotes Glucose Metabolism. *Sci. Rep.* **5**, 15981 (2015).

43. M. Elschami, M. Scherr, B. Philippens, R. Gerardy-Schahn, Reduction of STAT3 expression induces mitochondrial dysfunction and autophagy in cardiac HL-1 cells. *Eur. J. Cell Biol.* **92**, 21-29 (2013).

44. K. Szczepanek, A. Xu, Y. Hu, J. Thompson, J. He, A. C. Larner, F. N. Salloum, Q. Chen, E. J. Lesnefsky, Cardioprotective function of mitochondrial-targeted and transcriptionally inactive STAT3 against ischemia and reperfusion injury. *Basic Res. Cardiol.* **110**, 53-015-0509-2. Epub 2015 Sep 11 (2015).

45. K. Szczepanek, Q. Chen, M. Derecka, F. N. Salloum, Q. Zhang, M. Szelag, J. Cichy, R. C. Kukreja, J. Dulak, E. J. Lesnefsky, A. C. Larner, Mitochondrial-targeted Signal transducer and activator of transcription 3 (STAT3) protects against ischemia-induced changes in the electron transport chain and the generation of reactive oxygen species. *J. Biol. Chem.* **286**, 29610-29620 (2011).

46. K. Boengler, A. Buechert, Y. Heinen, C. Roeskes, D. Hilfiker-Kleiner, G. Heusch, R. Schulz, Cardioprotection by ischemic postconditioning is lost in aged and STAT3-deficient mice. *Circ. Res.* **102**, 131-135 (2008).

47. C. Capron, K. Jondeau, L. Casetti, V. Jalbert, C. Costa, E. Verhoeyen, J. M. Masse, P. Coppo, M. C. Bene, P. Bourdoncle, E. Cramer-Borde, I. Dusanter-Fourt, Viability and stress protection of chronic lymphoid leukemia cells involves overactivation of mitochondrial phosphoSTAT3Ser727. *Cell. Death Dis.* **5**, e1451 (2014).

48. D. J. Gough, I. J. Marie, C. Lobry, I. Aifantis, D. E. Levy, STAT3 supports experimental K-RasG12D-induced murine myeloproliferative neoplasms dependent on serine phosphorylation. *Blood.* (2014).

49. G. G. Mackenzie, L. Huang, N. Alston, N. Ouyang, K. Vrankova, G. Mattheolabakis, P. P. Constantinides, B. Rigas, Targeting mitochondrial STAT3 with the novel phospho-

valproic acid (MDC-1112) inhibits pancreatic cancer growth in mice. *PLoS One.* **8**, e61532 (2013).

50. R. Qureshi, O. Yildirim, A. Gasser, C. Basmadjian, Q. Zhao, J. P. Wilmet, L. Desaubry, C. G. Nebigil, FL3, a Synthetic Flavagline and Ligand of Prohibitins, Protects Cardiomyocytes via STAT3 from Doxorubicin Toxicity. *PLoS One.* **10**, e0141826 (2015).

51. E. Carbognin, R. M. Betto, M. E. Soriano, A. G. Smith, G. Martello, Stat3 promotes mitochondrial transcription and oxidative respiration during maintenance and induction of naive pluripotency. *EMBO J.* **35**, 618-634 (2016).

52. P. C. Cogswell, D. F. Kashatus, J. A. Keifer, D. C. Guttridge, J. Y. Reuther, C. Bristow, S. Roy, D. W. Nicholson, A. S. Baldwin Jr, NF-kappa B and I kappa B alpha are found in the mitochondria. Evidence for regulation of mitochondrial gene expression by NF-kappa B. *J. Biol. Chem.* **278**, 2963-2968 (2003).

53. S. Murase, Signal transducer and activator of transcription 3 (STAT3) degradation by proteasome controls a developmental switch in neurotrophin dependence. *J. Biol. Chem.* **288**, 20151-20161 (2013).

54. A. Bayot, M. Gareil, L. Chavatte, M. P. Hamon, C. L'Hermitte-Stead, F. Beaumatin, M. Priault, P. Rustin, A. Lombes, B. Friguet, A. L. Bulteau, Effect of Lon protease knockdown on mitochondrial function in HeLa cells. *Biochimie.* **100**, 38-47 (2014).

55. V. Soubannier, G. L. McLelland, R. Zunino, E. Braschi, P. Rippstein, E. A. Fon, H. M. McBride, A vesicular transport pathway shuttles cargo from mitochondria to lysosomes. *Curr. Biol.* **22**, 135-141 (2012).

56. G. L. McLelland, V. Soubannier, C. X. Chen, H. M. McBride, E. A. Fon, Parkin and PINK1 function in a vesicular trafficking pathway regulating mitochondrial quality control. *EMBO J.* **33**, 282-295 (2014).

57. A. Sugiura, G. L. McLelland, E. A. Fon, H. M. McBride, A new pathway for mitochondrial quality control: mitochondrial-derived vesicles. *EMBO J.* **33**, 2142-2156 (2014).

58. C. C. Su, J. Y. Yang, H. B. Leu, Y. Chen, P. H. Wang, Mitochondrial Akt-regulated mitochondrial apoptosis signaling in cardiac muscle cells. *Am. J. Physiol. Heart Circ. Physiol.* **302**, H716-23 (2012).

59. A. Rasola, M. Sciacovelli, F. Chiara, B. Pantic, W. S. Brusilow, P. Bernardi, Activation of mitochondrial ERK protects cancer cells from death through inhibition of the permeability transition. *Proc. Natl. Acad. Sci. U. S. A.* **107**, 726-731 (2010).

60. N. Hanawa, M. Shinohara, B. Saberi, W. A. Gaarde, D. Han, N. Kaplowitz, Role of JNK translocation to mitochondria leading to inhibition of mitochondria bioenergetics in acetaminophen-induced liver injury. *J. Biol. Chem.* **283**, 13565-13577 (2008).

61. G. N. Bijur, R. S. Jope, Rapid accumulation of Akt in mitochondria following phosphatidylinositol 3-kinase activation. *J. Neurochem.* **87**, 1427-1435 (2003).

62. P. Tammineni, C. Anugula, F. Mohammed, M. Anjaneyulu, A. C. Larner, N. B. Sepuri, The import of the transcription factor STAT3 into mitochondria depends on GRIM-19, a component of the electron transport chain. *J. Biol. Chem.* (2012).

63. A. M. Nargund, M. W. Pellegrino, C. J. Fiorese, B. M. Baker, C. M. Haynes, Mitochondrial import efficiency of ATFS-1 regulates mitochondrial UPR activation. *Science.* **337**, 587-590 (2012).

64. X. Wang, X. J. Chen, A cytosolic network suppressing mitochondria-mediated proteostatic stress and cell death. *Nature.* **524**, 481-484 (2015).

65. S. Senturk, Z. Yao, M. Camiolo, B. Stiles, T. Rathod, A. M. Walsh, A. Nemajerova, M. J. Lazzara, N. K. Altorki, A. Krainer, U. M. Moll, S. W. Lowe, L. Cartegni, R. Sordella, p53Psi is a transcriptionally inactive p53 isoform able to reprogram cells toward a metastatic-like state. *Proc. Natl. Acad. Sci. U. S. A.* **111**, E3287-96 (2014).

66. D. L. Hevehan, W. M. Miller, E. T. Papoutsakis, Differential expression and phosphorylation of distinct STAT3 proteins during granulocytic differentiation. *Blood.* **99**, 1627-1637 (2002).

67. G. Sutendra, A. Kinnaird, P. Dromparis, R. Paulin, T. H. Stenson, A. Haromy, K. Hashimoto, N. Zhang, E. Flaim, E. D. Michelakis, A nuclear pyruvate dehydrogenase complex is important for the generation of acetyl-CoA and histone acetylation. *Cell.* **158**, 84-97 (2014).

68. K. Tan, M. Fujimoto, R. Takii, E. Takaki, N. Hayashida, A. Nakai, Mitochondrial SSBP1 protects cells from proteotoxic stresses by potentiating stress-induced HSF1 transcriptional activity. *Nat. Commun.* **6**, 6580 (2015).

69. A. M. Nargund, C. J. Fiorese, M. W. Pellegrino, P. Deng, C. M. Haynes, Mitochondrial and nuclear accumulation of the transcription factor ATFS-1 promotes OXPHOS recovery during the UPR(mt). *Mol. Cell.* **58**, 123-133 (2015).

70. M. W. Pellegrino, A. M. Nargund, C. M. Haynes, Signaling the mitochondrial unfolded protein response. *Biochim. Biophys. Acta.* **1833**, 410-416 (2013).

71. P. M. Quiros, A. Mottis, J. Auwerx, Mitonuclear communication in homeostasis and stress. *Nat. Rev. Mol. Cell Biol.* **17**, 213-226 (2016).

72. M. Tavecchio, S. Lisanti, A. Lam, J. C. Ghosh, N. M. Martin, M. O'Connell, A. T. Weeraratna, A. V. Kossenkov, L. C. Showe, D. C. Altieri, Cyclophilin D Extramitochondrial Signaling Controls Cell Cycle Progression and Chemokine-Directed Cell Motility. *J. Biol. Chem.* (2013).

73. O. A. Timofeeva, V. Gaponenko, S. J. Lockett, S. G. Tarasov, S. Jiang, C. J. Michejda, A. O. Perantoni, N. I. Tarasova, Rationally designed inhibitors identify STAT3 N-domain as a promising anticancer drug target. *ACS Chem. Biol.* **2**, 799-809 (2007).

74. A. Ostman, J. Frijhoff, A. Sandin, F. D. Bohmer, Regulation of protein tyrosine phosphatases by reversible oxidation. *J. Biochem.* **150**, 345-356 (2011).

75. R. J. Salmond, D. R. Alexander, SHP2 forecast for the immune system: fog gradually clearing. *Trends Immunol.* **27**, 154-160 (2006).

76. S. J. Park, H. Y. Kim, H. Kim, S. M. Park, E. H. Joe, I. Jou, Y. H. Choi, Oxidative stress induces lipid-raft-mediated activation of Src homology 2 domain-containing protein-tyrosine phosphatase 2 in astrocytes. *Free Radic. Biol. Med.* **46**, 1694-1702 (2009).

77. H. Zheng, S. Li, P. Hsu, C. K. Qu, Induction of a tumor-associated activating mutation in protein tyrosine phosphatase Ptpn11 (Shp2) enhances mitochondrial metabolism, leading to oxidative stress and senescence. *J. Biol. Chem.* **288**, 25727-25738 (2013).

78. A. Bigi, E. Beltrami, M. Trinei, M. Stendardo, P. G. Pelicci, M. Giorgio, Cyclophilin D counteracts P53-mediated growth arrest and promotes Ras tumorigenesis. *Oncogene.* (2016).

79. A. V. Vaseva, N. D. Marchenko, K. Ji, S. E. Tsirka, S. Holzmann, U. M. Moll, P53 Opens the Mitochondrial Permeability Transition Pore to Trigger Necrosis. *Cell.* **149**, 1536-1548 (2012).

80. C. Mertens, B. Haripal, S. Klinge, J. E. Darnell, Mutations in the linker domain affect phospho-STAT3 function and suggest targets for interrupting STAT3 activity. *Proc. Natl. Acad. Sci. U. S. A.* **112**, 14811-14816 (2015).

81. M. R. Wieckowski, C. Giorgi, M. Lebiedzinska, J. Duszynski, P. Pinton, Isolation of mitochondria-associated membranes and mitochondria from animal tissues and cells. *Nat. Protoc.* **4**, 1582-1590 (2009).

82. M. Derecka, A. Gornicka, S. B. Koralov, K. Szczepanek, M. Morgan, V. Raje, J. Sisler, Q. Zhang, D. Otero, J. Cichy, K. Rajewsky, K. Shimoda, V. Poli, B. Strobl, S. Pellegrini, T. E. Harris, P. Seale, A. P. Russell, A. J. McAinch, P. E. O'Brien, S. R. Keller, C. M. Croniger, T. Kordula, A. C. Larner, Tyk2 and Stat3 regulate brown adipose tissue differentiation and obesity. *Cell. Metab.* **16**, 814-824 (2012).

83. J. D. Sisler, M. Morgan, V. Raje, R. C. Grande, M. Derecka, J. Meier, M. Cantwell, K. Szczepanek, W. J. Korzun, E. J. Lesnefsky, T. E. Harris, C. M. Croniger, A. C. Larner, The Signal Transducer and Activator of Transcription 1 (STAT1) Inhibits Mitochondrial Biogenesis in Liver and Fatty Acid Oxidation in Adipocytes. *PLoS One.* **10**, e0144444 (2015).

84. Y. Benjamini, Y. Hochberg, Controlling the False Discovery Rate: A practical and Powerful Approach to Multiple Testing. *Journal of the Royal Statistical Society. Series B (Methodological)*. **57**, 289-300 (1995).

ACKNOWLEDGEMENTS: We would like to thank Dr. Tomasz Kordula (Virginia Commonwealth University), Dr. Ed Lesnefsky (Virginia Commonwealth University), Dr. Gerald Shadel (Yale University), Dr. James E. Darnell (Rockefeller University), Dr. Georg Auburger (Goethe University Medical School), Dr. David Kashatus (University of Virginia), Dr. Thurl Harris (University of Virginia), and Dr. David Brautigan (University of Virginia) for their helpful advice and invaluable discussions regarding this work. We would also like to thank Drs. Gordon Ginder, Charles Clevenger, and Frank Fang, Virginia Commonwealth University; Dr. Swati Deb, Virginia Commonwealth University; Dr. Thurl Harris, University of Virginia; Dr. Ute Moll, Stony Brook University; Dr. Georg Auburger, Goethe – Universität; Heinz Baumann, Roswell Park Cancer Institute; Dr. Ed Lesnefsky, Virginia Commonwealth University; and Claudia Mertens, Rockefeller University for providing cell lines, plasmids, and reagents. We would also like to thank Julie Farnsworth and Qingzhao Zhang in the Flow Cytometry core for their continuous help in the generation of stable cell lines used for these studies. **Funding:** This research was supported by NIH-NIGMS R01 GM101677 to ACL, Massey Cancer Center 2013-

MIP-03 to ACL and KT, and NIH-NCI F30 CA183175 to JAM. Further research support to KT is also through funding from NIH-NCI (R01CA160688) and the Susan G. Komen Foundation (Investigator Initiated Research Grant, IIR12222224). Support to PES by the British Heart Foundation grant Nos. FS/11/58/28937 and FS/15/43/31565. Additional support was provided by CTSA award No. UL1TR000058 from the National Center for Advancing Translational Sciences. Services and products in support of the research project were generated by the VCU Massey Cancer Center Flow Cytometry Shared Resource, supported, in part, with funding from NIH-NCI Cancer Center Support Grant P30 CA016059. Microscopy was performed at the VCU Microscopy Facility, supported, in part, by funding from NIH-NCI Cancer Center Support Grant P30 CA016059. **Author Contributions:** J.A.M., M.H., M.C., A.R., C.M., V.R., J.S., E.T., S.T-O., S.G., and D.P. performed the experiments, and collected and analyzed the data. J.A.M., M.H., P.E.S., H.B., K.T., and A.C.L. conceived and planned the experiments. J.A.M. and A.C.L. wrote the manuscript. **Competing Interests:** The authors declare that they have no competing interests.

FIGURE LEGENDS

Figure 1: Oxidative Stress Triggers a Loss of Mitochondrial STAT3. Wild-type (WT) MEFs or 4T1 cells were treated with 1mM H_2O_2 for the indicated times and mitochondrial (mito) (**A**) or cytosolic (cyto) (**B**) extracts were probed for STAT3. Quantification of mitoSTAT3 as compared to a loading control is depicted in (**A**). *$p<0.05$ (compared to control), ; #$p<0.05$ (compared to control). Blots are representative

of 3 independent experiments. (**C**) WT MEFs treated with the indicated concentrations of H_2O_2 and extracts probed for mitoSTAT3 (top panel) and phosphorylated (p) Tyr^{705} and total STAT3 in the cytosol (bottom panel) (Tubulin: cytosolic loading control; CypD: mitochondrial loading control). Blots are representative of 2 independent experiments. (**D**) Isolated mitochondria from WT MEFs treated for the indicated times with H_2O_2 were immunoblotted for mitoSTAT3 or mitoSTAT1 and quantified. *$p<0.01$, **$p<0.04$, #$p<0.005$. Blots are representative of 3 independent experiments. (**E)** MDA-231 and SK-BR3 human breast cancer cells were treated for the indicated times with H_2O_2 and immunoblotted for STAT3 and GRIM19 (mitochondrial loading control). Blots are representative of 2 independent experiments. (**F**) WI-38 human lung fibroblasts were treated with H_2O_2 and purified mitochondria were immediately lysed in sample buffer. Blots were probed for mitoSTAT3, pERK1/2, and NDUFA9 (mitochondrial loading control). Blots are representative of 2 independent experiments.

Figure 2: Cytokine Treatment of Cells Induces mitoSTAT3 Loss and Recovery. (A and B) WT MEFs were treated with either OSM (**A**) and IL-6 (**B**) for the indicated times and mitochondrial extracts were immunoblotted for STAT3, pERK, tERK, and a loading control (NDUFA9 and/or CypD) (top panels). Cytosolic extracts probed for $pTyr^{705}$ STAT3 are shown to confirm cell activation (lower panels). Blots are representative of 2 independent experiments. (**C**) Mitochondria from 4T1 cells treated with OSM (upper panel) or MDA-231 cells treated with IL-6 (bottom panel) were probed for STAT3 and loading control (GRIM19 or CypD). Blots are representative of 2 independent experiments. (**D**) Rat hepatoma cell lines expressing the chimeric GCSF-

gp130 receptor were stimulated with recombinant human GCSF and immunoblotted for STAT3 in the mitochondrial fraction or pTyr^{705} STAT3 in the cytosolic fraction. Blots are representative of 2 independent experiments. (**E**) Purified mitochondria (P-Mito) from control or OSM stimulated WT MEFs were fractionated into cytosolic (cyto), ER (endoplasmic reticulum), crude mitochondria (C-mito), pure mitochondria (P-mito), and a mitochondrial associated membrane fraction (MAM) and blotted against a total homogenate fraction (Homog.). The abundance of Calreticulin (ER and MAM marker), Tubulin (cytosolic marker), NDUFA9 (mitochondrial marker), Histone H3 (nuclear marker), and STAT3 is shown. Blots are representative of 2 independent experiments

.

Figure 3: Inhibition of JAKs Prevents mitoSTAT3 Loss Upon Cytokine Treatment. (A and B) MEFs were incubated with or without the JAK inhibitor ruxolitinib for 1H prior to the addition of OSM (**A**) or H_2O_2 (**B**), and mitochondrial and cytosolic extracts were immunoblotted for STAT3 or pTyr^{705} STAT3 respectively. Blots are representative of 3 independent experiments. Densitometric quantification of mitochondrial results from (**A**) is depicted. * $p<0.01$, # $p<0.001$, ns=not significant. (**C**) Mitochondria were isolated from MDA231 breast cancer cells treated with ruxolitinib for 1H prior to the addition of OSM or H_2O_2 for the indicated times and immunoblotted for STAT3 and NDUFA9 (loading control). Blots are representative of 2 independent experiments. (**D**) Mitochondrial superoxide production was assayed by flow cytometry analysis using the MitoSOX dye in WT MEFs treated for 30' with either OSM or H_2O_2. *p=0.0002, **p=0.0002. N=3 independent experiments. (**E**) WT MEFs were pre-treated for 1H with the mitochondrial restricted anti-oxidant mitoTEMPO and then stimulated for 30' with

H_2O_2 with mitochondrial extracts blotted for STAT3, pERK1/2, or NDUFA9 (loading control). Blots are representative of two independent experiments. (**F**) WT MEFs were pre-treated with the MEK inhibitor PD0325901 for 1H followed by H_2O_2 treatment for the indicated times and isolated mitochondria were subjected to SDS-PAGE and immunoblotted for STAT3, pERK1/2, tERK1/2, and NDUFA9 (loading control). Blots are representative of 2 independent experiments.

Figure 4: Recovery of mitoSTAT3 is Dependent on New Protein Synthesis and S727 Phosphorylation of STAT3. A) *STAT3*$^{-/-}$ MEFs were engineered to stably express mitochondrial targeted STAT3 (MLS-STAT3) and subjected to H_2O_2 treatment. Whole cell extract (WCE) and mitochondria were western blotted for STAT3 or the respective loading control. Blots are representative of 3 independent experiments and densitometric quantification is shown. (**B**) Mitochondria from MDA-231 cells were pre-treated for 4H with vehicle or MG132 and treated with OSM or H_2O_2 and extracts probed for STAT3. Cytosolic extracts from vehicle or MG132 treated cells were probed for Ubiquitin (Ub) (right panel). Blots are representative of 2 independent experiments. (**C and D**) Mitochondrial extracts from MDA-231 cells treated with or without cycloheximide and stimulated with OSM or H_2O_2 were subjected to western blotting (C). Results from OSM experiments were quantified in (**D**) by densitometry analysis. *p=0.009; #p=0.023, ns=not significant. N=3 independent experiments. (**E and F**) *STAT3*$^{-/-}$ MEFs expressing WT STAT3 (STAT3α) or the nonphosphorylatable mutant (STAT3 S727A) were treated for the indicated times with OSM and mitochondrial lysates were immunoblotted for

STAT3 (E). Quantification of these results are presented in (**F**). *p<0.005; #p≤0.0002, **p<0.002, ***p<0.02, ns=not significant. N=3 independent experiments.

Figure 5: mitoSTAT3 Interacts with CypD. (**A**) Lysates from WT MEF whole cell extracts treated with H_2O_2 were subjected to pulldown with bead-bound GST-CypD (coomassie stain) and probed for STAT3 (Input, lower panels). Blots are representative of 2 independent experiments. (**B and C**) WT MEFs (B) and 4T1 cells (C) were incubated with H_2O_2 for various times prior to isolation of mitochondria. Extracts were incubated with GST-CypD in the presence (lane 6) or absence of CsA and STAT3 was assayed by immunoblots (upper panels). Lower panels show the input (10% of that used for the pull downs). Blots are representative of 2 independent experiments. (**D**) Mitochondria from 4T1 cells either untreated or treated with H_2O_2 were subjected to GST-CypD or GST pull-down with immunoblotting for STAT3 or GST. Input is shown in the lower panels. Blots are representative of 2 independent experiments. (**E**) MitoSTAT3 immunoprecipitations (IPs) from MEFs and 4T1 cells treated 30 min with H_2O_2. Immunoblots were probed for STAT3 (lower panels) or CypD (upper panels). Input (10% of that used for immunoprecipitation) is shown. Blots are representative of 2 independent experiments. (**F**) GST-CypD pulldown of mitochondrial extracts from MDA-231 cells treated with IL-6 and the soluble IL-6Rα with input shown below. Blots were probed for STAT3. ATP5O is shown as a loading control for the pulldown and input samples.

Figure 6: Binding of mitoSTAT3 to CypD is Mediated through STAT3's N-terminus and can be re-capitulated in a cell free system.

(**A**) 293T cells expressing various chimeric versions of Flag tagged STAT3/STAT1 were treated with H_2O_2 and whole cell extracts were incubated with GST-CypD and probed for Flag (upper panel). Lower panels show the input (10% of that used for the pull downs) with coomassie stain of the GST-CypD input. Blots are representative of 3 independent experiments. (**B**) Diagram of the chimeric constructs used in (**A**) indicating the critical region (green bar) in STAT3 that mediates its binding to CypD (13). (**C**) 293T cells expressing STAT3/1S or STAT1/3S were treated with H_2O_2, subjected to GST-CypD pulldown and probed for Flag (pulldown: top panel, input: bottom panel). Blots are representative of 2 independent experiments. (**D**) 293T cell lysates expressing STAT3/1H were warmed to 30 degrees and incubated with either GST-CypD or GST alone and immunoblotted for Flag. CsA was incubated with warmed lysates to also show specificity of the interaction (lane 5). Bottom panel depicts Coomassie stain for GST-CypD and GST. Blots are representative of 2 independent experiments. (**E**) Mitochondrial lysates from MDA-231 cells tested in the cell free system were incubated at 30 degrees and a GST-CypD pulldown was performed in the presence or absence of CsA with immunoblotting for STAT3 and ATP5O. Blots are representative of 2 independent experiments. (**F**) Extracts from 293T cells expressing the chimeric protein STAT3/1H were warmed to 30^o in the established cell free system in the presence of vanadate (Na_3VO_4), calycunin A, or the pan-phosphatase inhibitor cocktail PhosSTOP (Roche). Lysates (left panel, input) were subjected to GST-CypD pulldown (right panel) and probed for Flag (STAT3). Coomassie stain of GST-CypD is shown (right panel, bottom) to confirm equal loading of recombinant CypD. Blots are representative of 2 independent experiments.

Figure 7: A Tyrosine Phosphatase Mediated Event Drives mitoSTAT3-CypD Interactions. (**A**) 293T cells expressing STAT3/1S were pre-treated with either Vanadate (Na_3VO_4) or Staurosporine followed by treatment with H_2O_2 for 1H. Untreated lysates were also subjected to λ phosphatase (phos) treatment or mock treatment. GST-CypD pulldown samples (top) and the corresponding input (bottom panels) were probed for Flag (STAT3) with the input also immunoblotted for Tubulin (loading control) and pERK1/2. Coomassie stain of GST-CypD is shown (bottom panel) to confirm equal loading of recombinant CypD. Blots are representative of 2 independent experiments. (**B**) Extracts from 293T cells expressing STAT3/1H were dialyzed prior to mock treatment (30^oC) with or without the addition of ATP (20mM). Staurosporine was included during the mock treatment period for lysates in lanes 4 and 5. Binding of STAT3 and CypD was assessed by GST-CypD pulldown. Blots are representative of 3 independent experiments. (**C**) Whole cell extracts from *STAT3*$^{-/-}$ MEFs were incubated with recombinant STAT3 on ice or either during ($+^{pre}$) or after ($+^{post}$) warming of the extract at 30^o for 30 min. Input (bottom panel) and GST-CypD pulldowns were probed for STAT3. Blots are representative of 3 independent experiments. (**D**) MDA-231 human cancer cells were pre-treated with CsA and then treated with OSM and mitochondrial lysates were probed for STAT3. Blots are representative of 2 independent experiments. (**E**) *CypD*$^{+/+}$ MEFs and *CypD*$^{-/-}$ MEFs were incubated with cycloheximide and mitoSTAT3 abundance were assessed from purified mitochondrial extracts. Blots are representative of 2 independent experiments. (**F**) WT, *STAT3*$^{-/-}$ MEFs, or *STAT3*$^{-/-}$ MEFs reconstituted with STAT3 WT or STAT3/1S were treated with H_2O_2, stained with mitoSOX, and then analyzed by flow

cytometry. Results are normalized to each respective untreated sample. *p<0.01, **p<0.001, #p=0.0005. N=5 independent experiments.

Figure 8: Model of mitoSTAT3 regulation. Upon initial stimulation (left panel) mitoSTAT3 and/or mitochondrial proteases (mitoproteases) are post-translationally modified that induces their association and leads to the proteolytic cleavage of mitoSTAT3. Presumably proteolytic fragments of mitoSTAT3 may be further degraded or may contribute to extra-mitochondrial signaling. With continued stimulation (right panel) new protein synthesis (either of STAT3 or a chaperone protein required for STAT3 mitochondrial targeting) couples with Ser^{727} phosphorylation of STAT3 to mediate targeting of STAT3 to the mitochondria. Likely, mitoSTAT3 is also tyrosine phosphorylated (pY, non-Tyr^{705} site). Following its import into the mitochondria, mitoSTAT3 is dephosphorylated by a protein tyrosine phosphatase (PTP). This facilitates its interaction with CypD, which is likely important for mitoSTAT3's proper folding and mitochondrial stability. This association determines ROS abundance and is also likely important for other downstream effects of mitoSTAT3 including regulation of the ETC and maintenance of the permeability transition pore (mitoSTAT3's actions). OMM, outer mitochondrial membrane, IMS, intermembrane space, IMM, inner mitochondrial membrane.

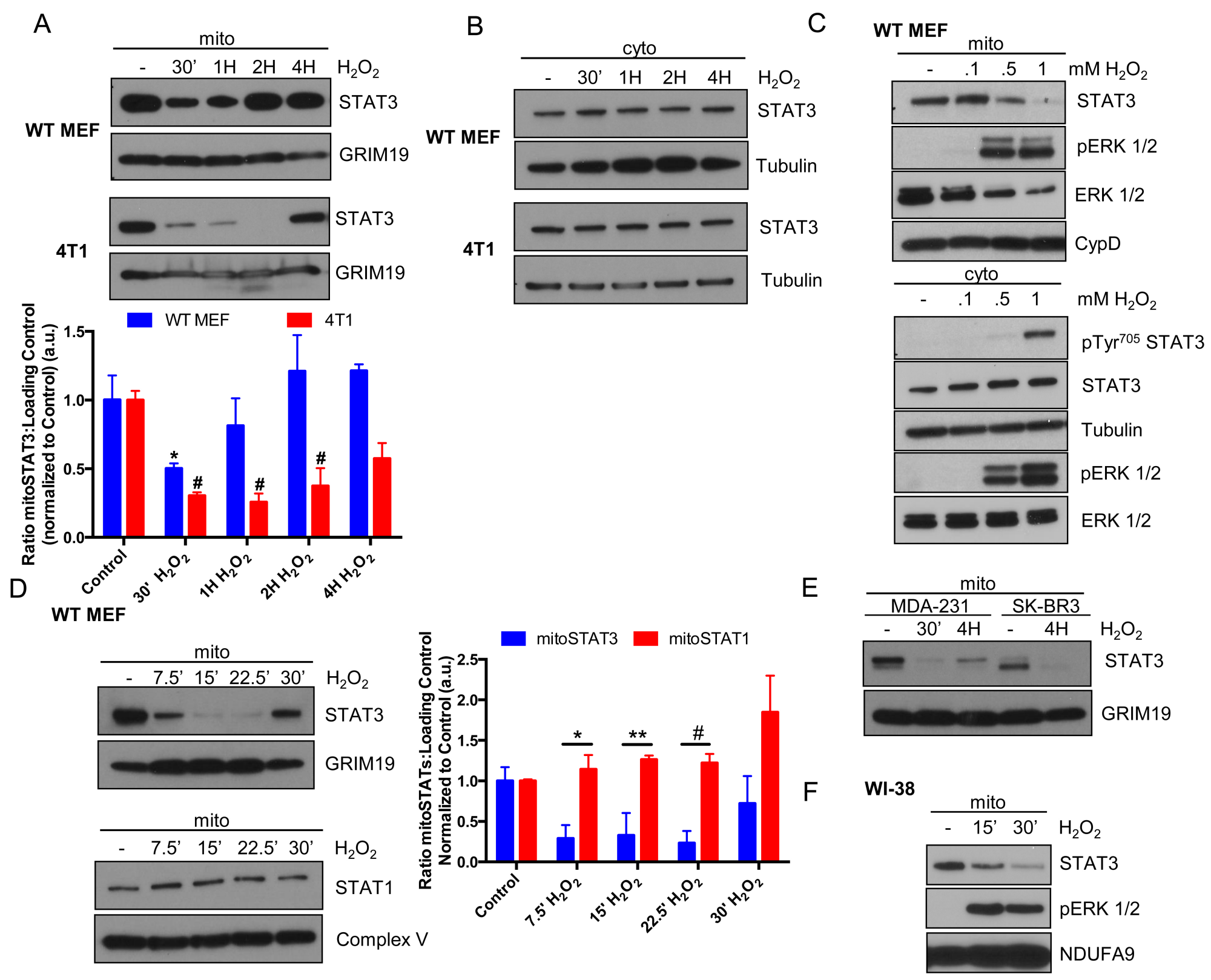
A
mito
- 30' 1H 2H 4H H_2O_2
WT MEF
STAT3
GRIM19
4T1
STAT3
GRIM19
WT MEF
4T1
Ratio mitoSTAT3:Loading Control (normalized to Control) (a.u.)
1.5
1.0
0.5
0.0
*
#
#
#
Control
30' H_2O_2
1H H_2O_2
2H H_2O_2
4H H_2O_2
B
cyto
- 30' 1H 2H 4H H_2O_2
WT MEF
STAT3
Tubulin
4T1
STAT3
Tubulin
C
WT MEF
mito
- .1 .5 1 mM H_2O_2
STAT3
pERK 1/2
ERK 1/2
CypD
cyto
- .1 .5 1 mM H_2O_2
pTyr705 STAT3
STAT3
Tubulin
pERK 1/2
ERK 1/2
D
WT MEF
mito
- 7.5' 15' 22.5' 30' H_2O_2
STAT3
GRIM19
mito
- 7.5' 15' 22.5' 30' H_2O_2
STAT1
Complex V
mitoSTAT3
mitoSTAT1
Ratio mitoSTATs:Loading Control Normalized to Control (a.u.)
2.5
2.0
1.5
1.0
0.5
0.0
*
**
#
Control
7.5' H_2O_2
15' H_2O_2
22.5' H_2O_2
30' H_2O_2
E
mito
MDA-231
SK-BR3
- 30' 4H - 4H H_2O_2
STAT3
GRIM19
F
WI-38
mito
- 15' 30' H_2O_2
STAT3
pERK 1/2
NDUFA9

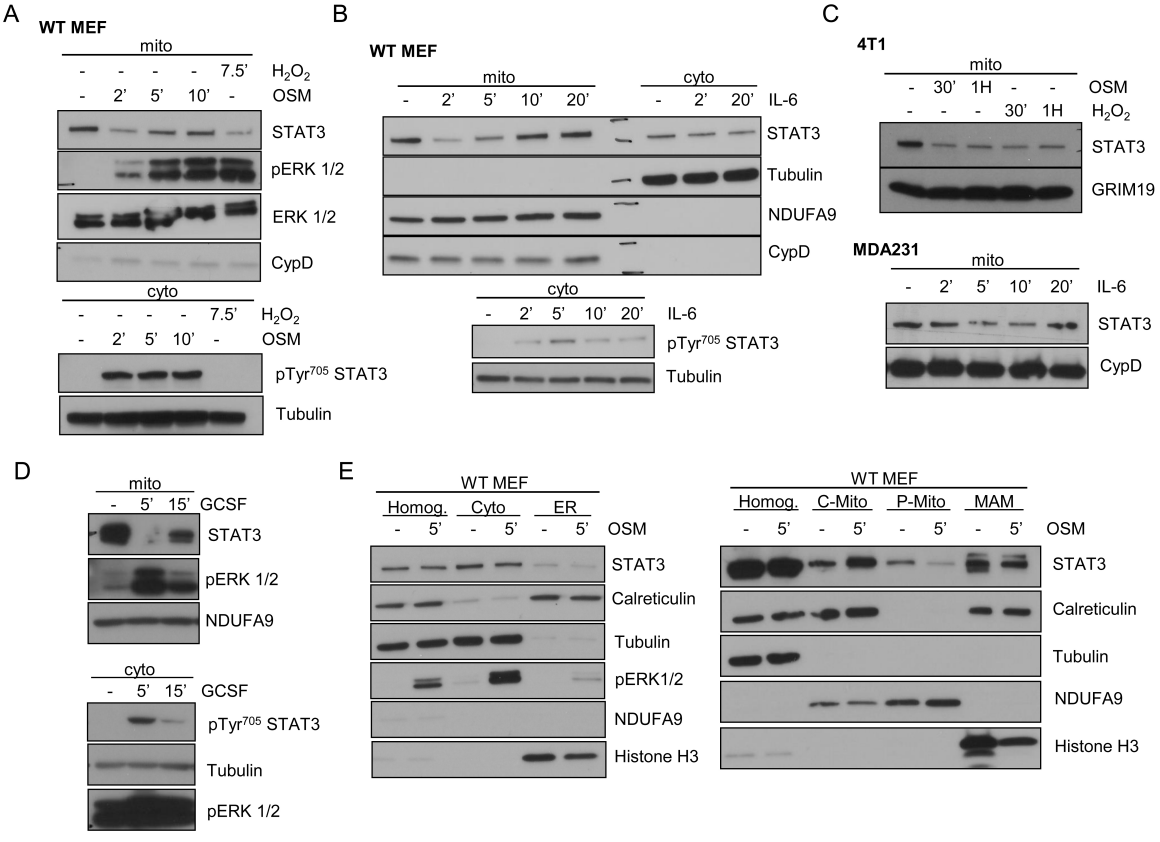
A
WT MEF
mito
- - - - 7.5' H2O2
- 2' 5' 10' - OSM
STAT3
pERK 1/2
ERK 1/2
CypD
cyto
- - - - 7.5' H2O2
- 2' 5' 10' - OSM
pTyr705 STAT3
Tubulin
B
WT MEF
mito
- 2' 5' 10' 20'
cyto
- 2' 20' IL-6
STAT3
Tubulin
NDUFA9
CypD
cyto
- 2' 5' 10' 20' IL-6
pTyr705 STAT3
Tubulin
C
4T1
mito
- 30' 1H - - OSM
- - - 30' 1H H2O2
STAT3
GRIM19
MDA231
mito
- 2' 5' 10' 20' IL-6
STAT3
CypD
D
mito
- 5' 15' GCSF
STAT3
pERK 1/2
NDUFA9
cyto
- 5' 15' GCSF
pTyr705 STAT3
Tubulin
pERK 1/2
E
WT MEF
Homog. Cyto ER
- 5' - 5' - 5' OSM
STAT3
Calreticulin
Tubulin
pERK1/2
NDUFA9
Histone H3
WT MEF
Homog. C-Mito P-Mito MAM
- 5' - 5' - 5' - 5' OSM
STAT3
Calreticulin
Tubulin
NDUFA9
Histone H3

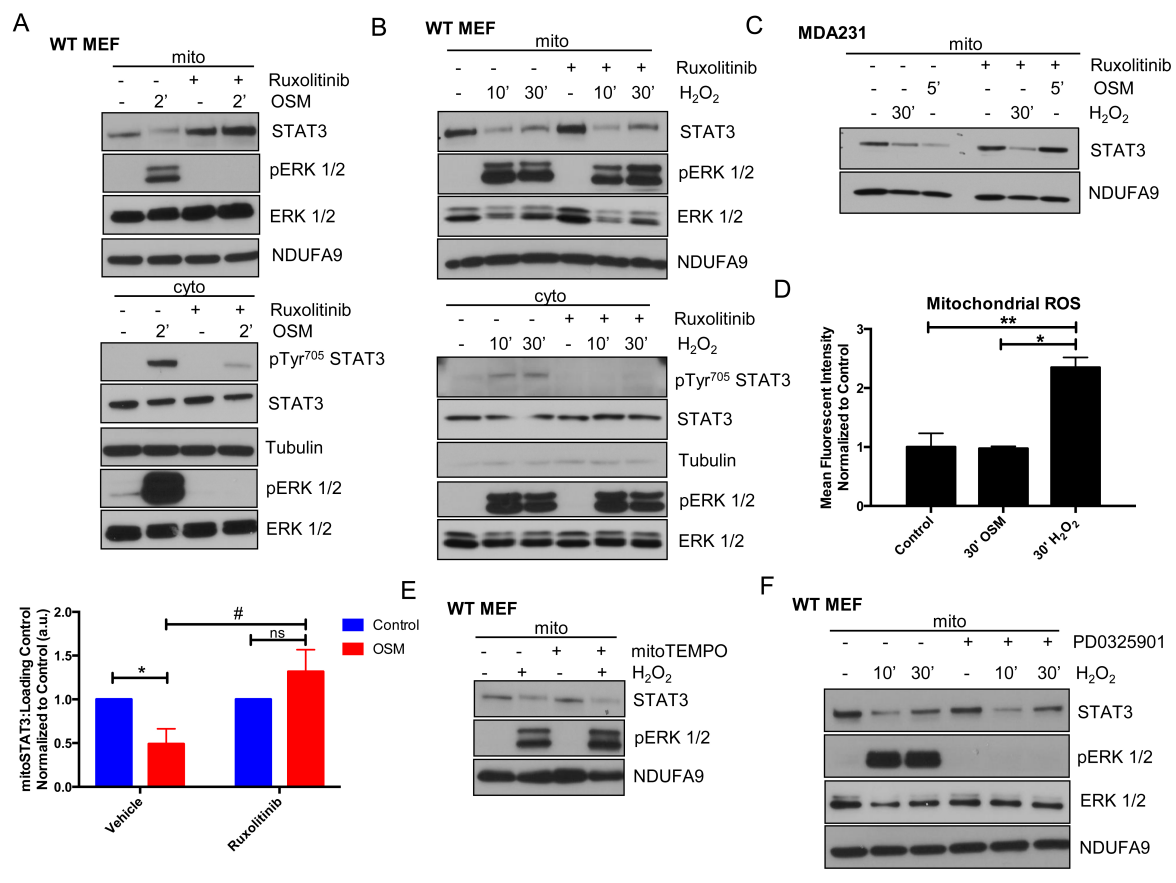
A
WT MEF
mito
Ruxolitinib
OSM
2'
STAT3
pERK 1/2
ERK 1/2
NDUFA9
cyto
pTyr705 STAT3
Tubulin
B
WT MEF
10'
30'
H2O2
C
MDA231
D
Mitochondrial ROS
Mean Fluorescent Intensity Normalized to Control
Control
30' OSM
30' H2O2
E
WT MEF
mitoTEMPO
mitoSTAT3:Loading Control Normalized to Control (a.u.)
Vehicle
Ruxolitinib
F
PD0325901

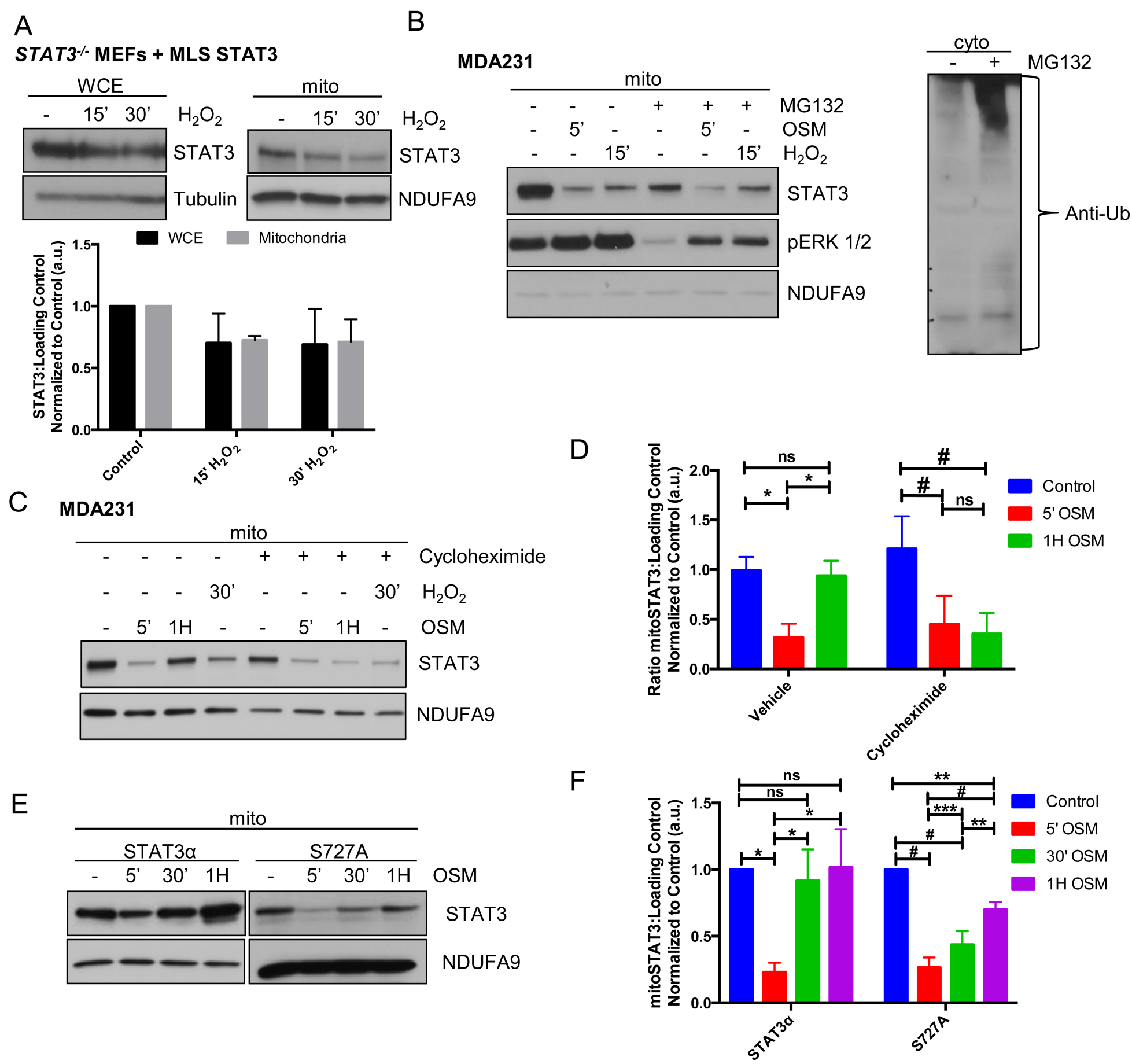
A
STAT3-/- MEFs + MLS STAT3
WCE
mito
- 15' 30' H2O2
STAT3
Tubulin
NDUFA9
WCE
Mitochondria
STAT3:Loading Control Normalized to Control (a.u.)
Control
15' H2O2
30' H2O2
B
MDA231
mito
MG132
OSM
H2O2
STAT3
pERK 1/2
NDUFA9
cyto
MG132
Anti-Ub
C
MDA231
mito
Cycloheximide
H2O2
OSM
STAT3
NDUFA9
D
Ratio mitoSTAT3:Loading Control Normalized to Control (a.u.)
Control
5' OSM
1H OSM
Vehicle
Cycloheximide
E
mito
STAT3α
S727A
OSM
STAT3
NDUFA9
F
mitoSTAT3:Loading Control Normalized to Control (a.u.)
Control
5' OSM
30' OSM
1H OSM
STAT3α
S727A

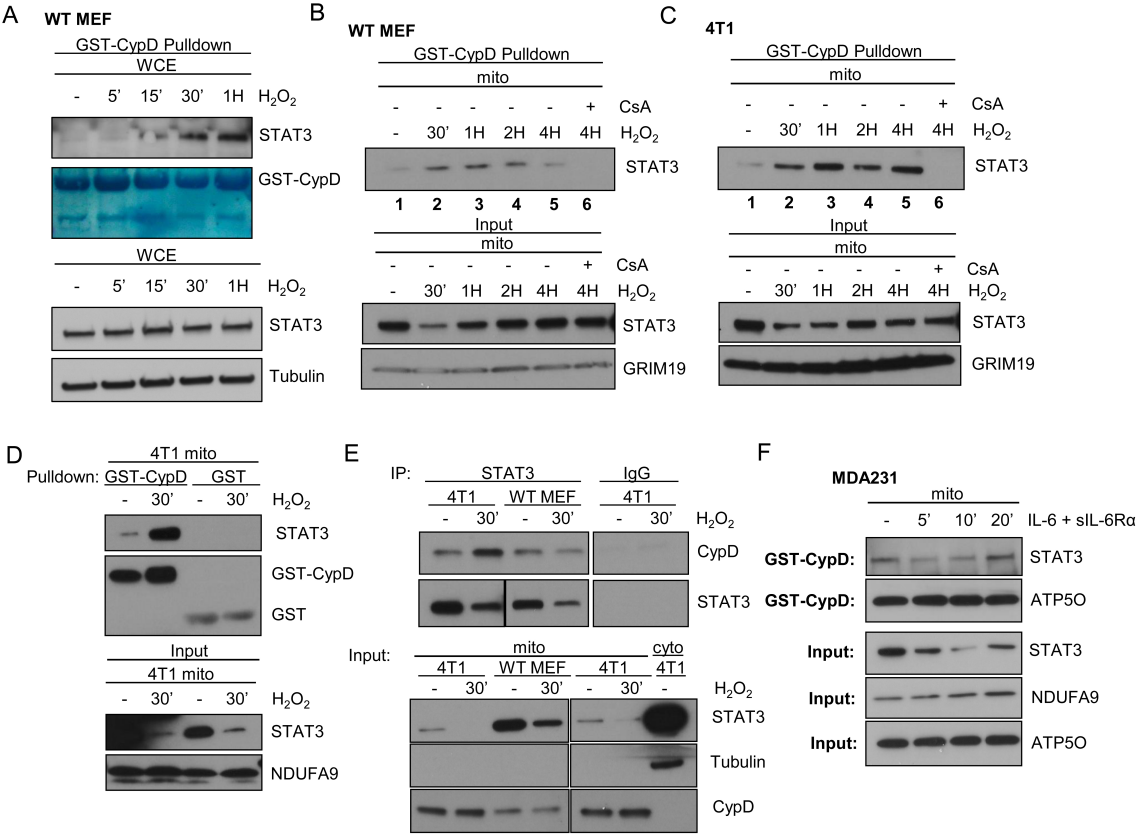
A
WT MEF
GST-CypD Pulldown
WCE
- 5' 15' 30' 1H H_2O_2
STAT3
GST-CypD
WCE
- 5' 15' 30' 1H H_2O_2
STAT3
Tubulin
B
WT MEF
GST-CypD Pulldown
mito
- - - - - + CsA
- 30' 1H 2H 4H 4H H_2O_2
STAT3
1 2 3 4 5 6
Input
mito
- - - - - + CsA
- 30' 1H 2H 4H 4H H_2O_2
STAT3
GRIM19
C
4T1
GST-CypD Pulldown
mito
- - - - - + CsA
- 30' 1H 2H 4H 4H H_2O_2
STAT3
1 2 3 4 5 6
Input
mito
- - - - - + CsA
- 30' 1H 2H 4H 4H H_2O_2
STAT3
GRIM19
D
4T1 mito
Pulldown: GST-CypD GST
- 30' - 30' H_2O_2
STAT3
GST-CypD
GST
Input
4T1 mito
- 30' - 30' H_2O_2
STAT3
NDUFA9
E
IP: STAT3 IgG
4T1 WT MEF 4T1
- 30' - 30' - 30' H_2O_2
CypD
STAT3
Input: mito cyto
4T1 WT MEF 4T1 4T1
- 30' - 30' - 30' -
H_2O_2
STAT3
Tubulin
CypD
F
MDA231
mito
- 5' 10' 20' IL-6 + sIL-6Rα
GST-CypD: STAT3
GST-CypD: ATP5O
Input: STAT3
Input: NDUFA9
Input: ATP5O

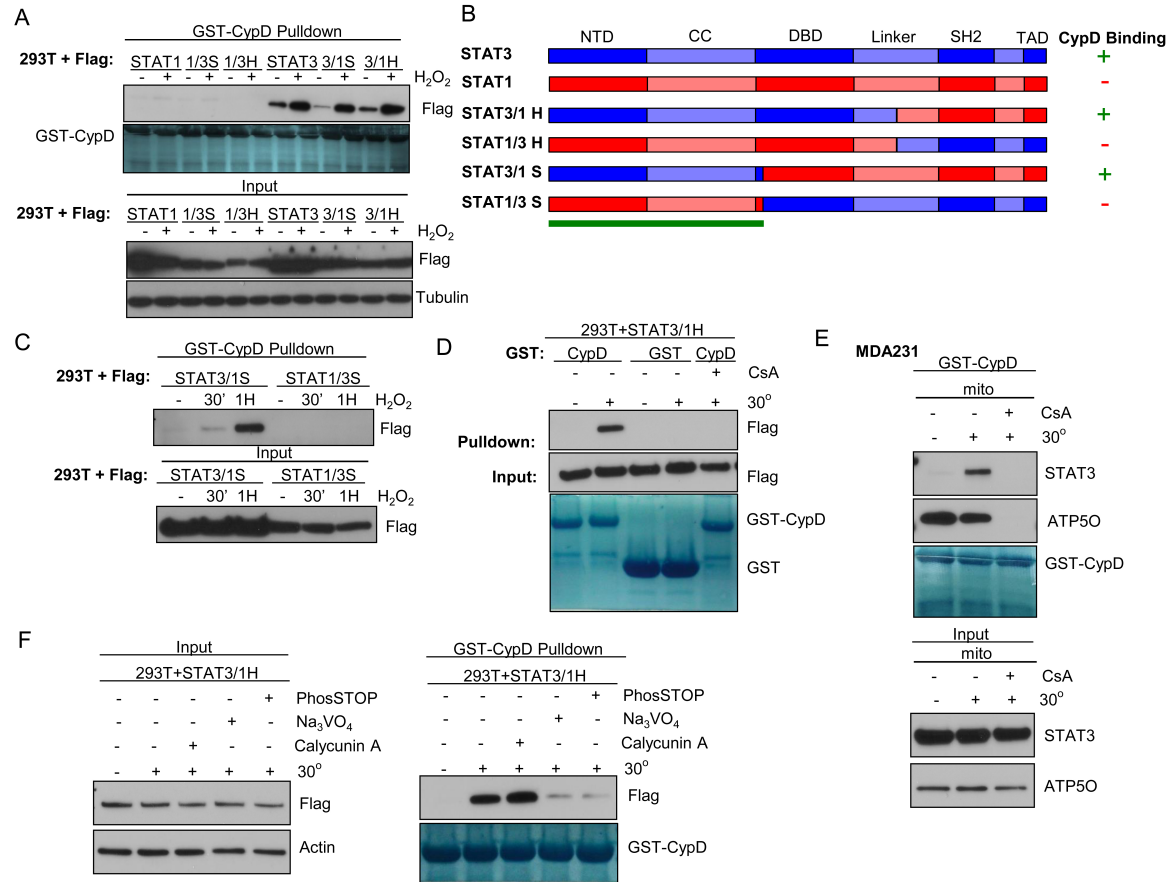
A
GST-CypD Pulldown
293T + Flag:
STAT1 1/3S 1/3H STAT3 3/1S 3/1H
H_2O_2
Flag
GST-CypD
Input
293T + Flag:
STAT1 1/3S 1/3H STAT3 3/1S 3/1H
H_2O_2
Flag
Tubulin
B
NTD CC DBD Linker SH2 TAD
CypD Binding
STAT3 +
STAT1 -
STAT3/1 H +
STAT1/3 H -
STAT3/1 S +
STAT1/3 S -
C
GST-CypD Pulldown
293T + Flag:
STAT3/1S STAT1/3S
30' 1H 30' 1H
H_2O_2
Flag
Input
293T + Flag:
STAT3/1S STAT1/3S
30' 1H 30' 1H
H_2O_2
Flag
D
293T+STAT3/1H
GST: CypD GST CypD
CsA
30°
Pulldown:
Flag
Input:
Flag
GST-CypD
GST
E
MDA231
GST-CypD
mito
CsA
30°
STAT3
ATP5O
GST-CypD
Input
mito
CsA
30°
STAT3
ATP5O
F
Input
293T+STAT3/1H
PhosSTOP
Na_3VO_4
Calycunin A
30°
Flag
Actin
GST-CypD Pulldown
293T+STAT3/1H
PhosSTOP
Na_3VO_4
Calycunin A
30°
Flag
GST-CypD

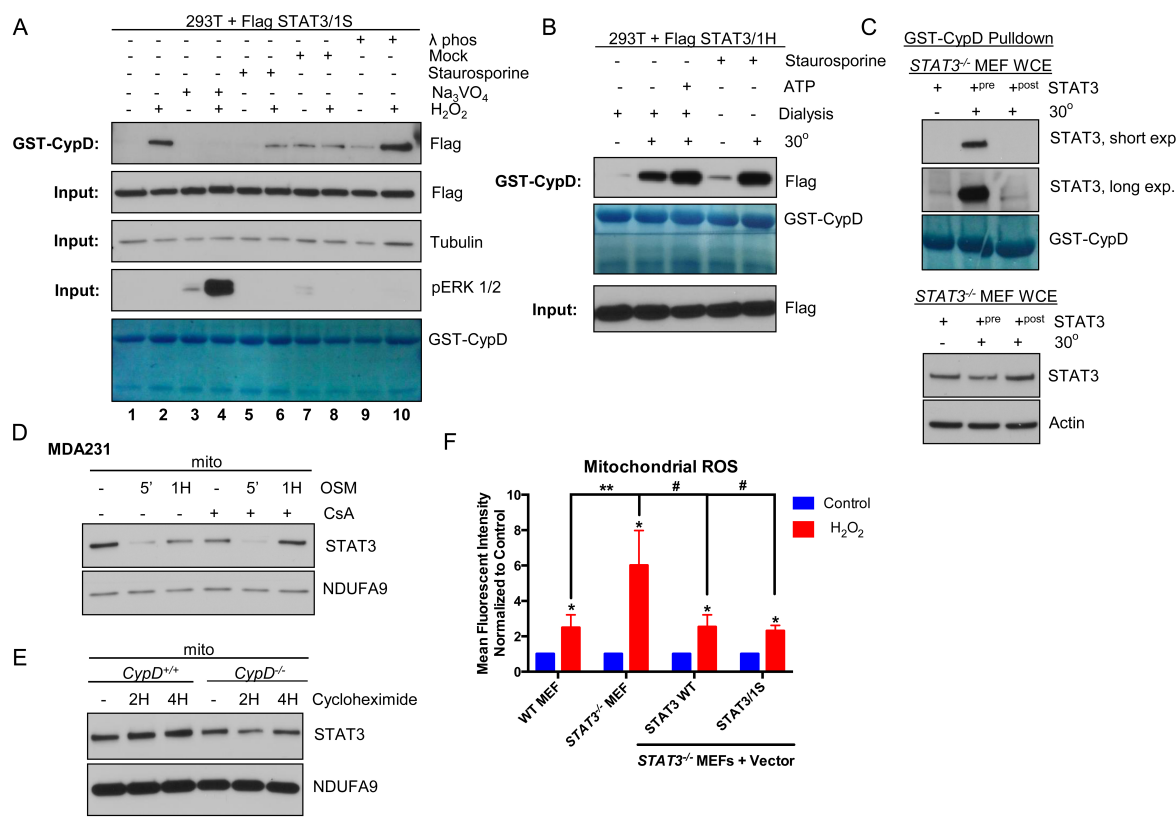
A
293T + Flag STAT3/1S
λ phos
Mock
Staurosporine
Na_3VO_4
H_2O_2
GST-CypD:
Flag
Input:
Flag
Input:
Tubulin
Input:
pERK 1/2
GST-CypD
1 2 3 4 5 6 7 8 9 10
B
293T + Flag STAT3/1H
Staurosporine
ATP
Dialysis
30°
GST-CypD:
Flag
GST-CypD
Input:
Flag
C
GST-CypD Pulldown
STAT3-/- MEF WCE
+pre
+post
STAT3
30°
STAT3, short exp
STAT3, long exp.
GST-CypD
STAT3-/- MEF WCE
STAT3
Actin
D
MDA231
mito
OSM
CsA
STAT3
NDUFA9
E
mito
CypD+/+
CypD-/-
Cycloheximide
STAT3
NDUFA9
F
Mitochondrial ROS
Mean Fluorescent Intensity Normalized to Control
Control
H_2O_2
WT MEF
STAT3-/- MEF
STAT3 WT
STAT3/1S
STAT3-/- MEFs + Vector

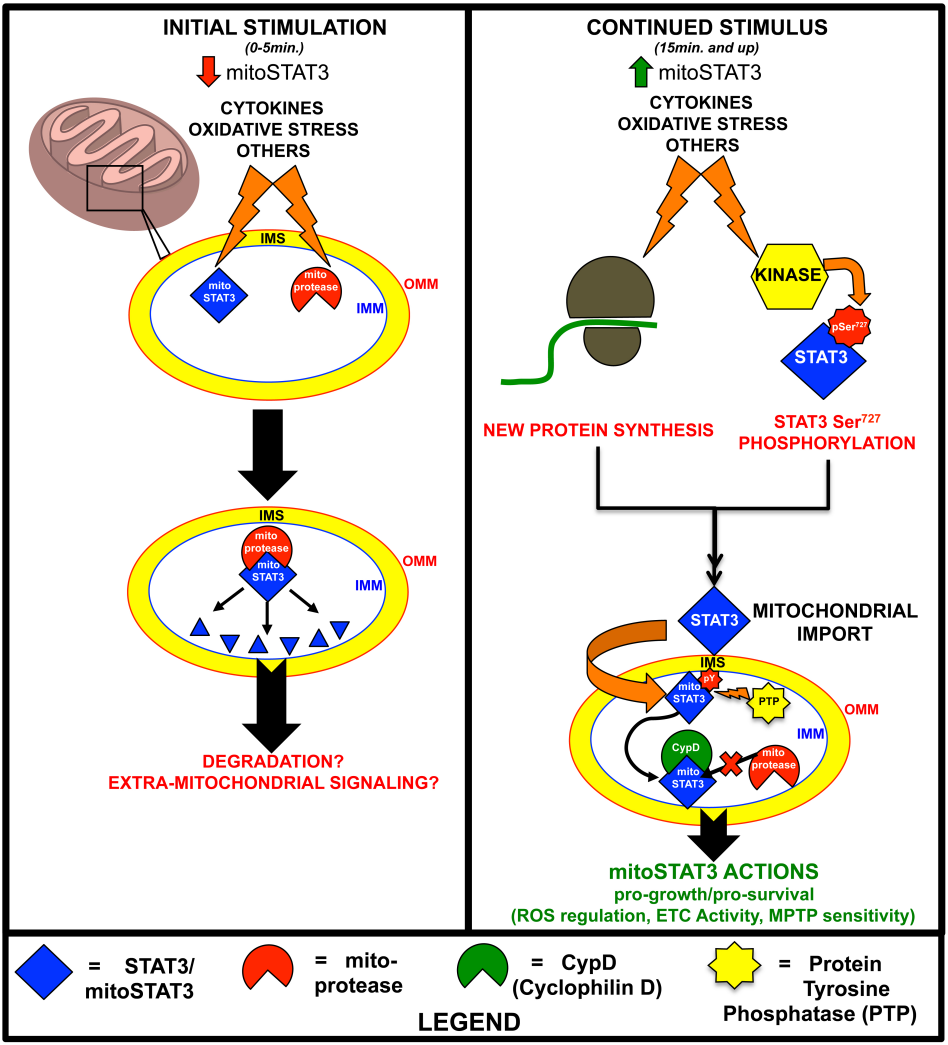
INITIAL STIMULATION
(0-5min.)
mitoSTAT3
CYTOKINES
OXIDATIVE STRESS
OTHERS
IMS
mito STAT3
mito protease
OMM
IMM
IMS
mito protease
mito STAT3
OMM
IMM
DEGRADATION?
EXTRA-MITOCHONDRIAL SIGNALING?
CONTINUED STIMULUS
(15min. and up)
mitoSTAT3
CYTOKINES
OXIDATIVE STRESS
OTHERS
KINASE
pSer727
STAT3
NEW PROTEIN SYNTHESIS
STAT3 Ser727 PHOSPHORYLATION
STAT3
MITOCHONDRIAL IMPORT
IMS
pY
mito STAT3
PTP
OMM
IMM
CypD
mito STAT3
mito protease
mitoSTAT3 ACTIONS
pro-growth/pro-survival
(ROS regulation, ETC Activity, MPTP sensitivity)
= STAT3/ mitoSTAT3
= mito-protease
= CypD (Cyclophilin D)
= Protein Tyrosine Phosphatase (PTP)
LEGEND